TRIBHUVAN UNIVERSITY
INSTITUTE OF ENGINEERING
PULCHOWK CAMPUS

B-11-BME-2018/2023

DESIGN AND FABRICATION OF SAVONIUS WIND TURBINE AND EXPERIMENTAL STUDY OF ITS USE IN A WATER PUMP.

By:
Bibish Chaulagain (075BME014)
Prashant Paudyal Sharma (075BME029)
Sandip Poudel (075BME039)

A PROJECT REPORT
SUBMITTED TO THE DEPARTMENT OF MECHANICAL AND AEROSPACE ENGINEERING IN PARTIAL FULFILLMENT OF THE REQUIREMENT FOR THE DEGREE OF BACHELOR IN MECHANICAL ENGINEERING

DEPARTMENT OF MECHANICAL AND AEROSPACE ENGINEERING
LALITPUR, NEPAL

APRIL, 2023

COPYRIGHT

TRIBHUVAN UNIVERSITY
INSTITUTE OF ENGINEERING
PULCHOWK CAMPUS
DEPARTMENT OF MECHANICAL AND AEROSPACE ENGINEERING

The undersigned certify that they have read, and recommended to the Institute of Engineering for acceptance, a project report entitled "Design and Fabrication of Savonius Wind Turbine and Experimental Study of its Use in a Water Pump" submitted by **Bibish Chaulagain**(075BME014), **Prashant Paudyal Sharma** (075BME029) and **Sandip Poudel** (075BME039) in partial fulfillment of the requirements for the degree of Bachelor of Mechanical Engineering.

Supervisor,Dr. Shree Raj Shakya
Associate Professor
Department of Mechanical and Aerospace Engineering

Supervisor,Tek Raj Subedi
Assistant Professor
Department of Mechanical and Aerospace Engineering

External Examiner
Dr.Iswor Bajracharya

Committee Chairperson
Dr. Surya Prasad Adhikari
Head,Department of Mechanical and Aerospace Engineering

Date

ABSTRACT

The utilization of wind power has been a sustainable way for renewable energy utilization in developing countries. The operation of water pump by wind energy has been used for many years. The project is about designing and fabricating a Helical Savonius wind turbine for water pumping application. The Helical Bach design was selected because of simplicity in design, producibility, efficient and able to operate at very low-wind conditions. The blade modeling was done in SolidWorks and analysis was done in ANSYS 2021. The fabrication process involves the selection of appropriate materials, design of rotor and shafts, followed by manufacturing and assembly of the components. The experimental study was done at the average wind speed ranging from 1.1 m/s to 4 m/s. The torque was measured using rope brake dynamometer setup. The CFD approach used for study at the wind speed of 4m/s and Tip speed ratio(TSR) of 0.32 calculates the coefficient of performance (Cp) to be 0.107 and in experimental found to be 0.025. The maximum average wind speed that the turbine was tested was 4 m/s with a rotational speed of 48.18 rpm. The cut-on speed was found to be 1 m/s. Overall, this project demonstrates the potential of Helical Savonius wind turbine for water pumping applications in low wind speed conditions thus facilitating the country for promoting indigenous and sustainable energy resources for low carbon development path.

ACKNOWLEDGEMENTS

We are grateful to the Department of Mechanical and Aerospace Engineering of Pulchowk Campus for providing us an opportunity to take upon a final year project.

We are highly indebted to our supervisor **Associate Professor Dr. Shree Raj Shakya** for his continuous guidance,motivation and assistance in carrying out this project.

We are sincerely thankful to our next supervisor **Assistant Professor Tek Raj Subedi** for his continuous support during experimental setup and providing facility for Simulation.

We would like to acknowledge **Assistant Professor Dr. Sudip Bhattarai** for his continuous support during simulation study of our project.

We would like to acknowledge **Center for Energy Studies,IOE** with much appreciation for assisting with the necessary equipment that are necessary for experimental study.

Our Sincere thanks to sir **Bal Mukunda Shrestha,Mr Mohan Tamang,Mr Shankhar Malla,Mr Ganesh Dhungana,Mr Pravesh Bhandari** for their valuable support during the fabrication and testing process.

Furthermore,we would also like to acknowledge with much appreciation the crucial role of various journals and research papers for providing us required information.

Our sincere gratitude towards all the people whose support and inspiration has been vital towards the success of this project.

TABLE OF CONTENTS

List of Figures

LIST OF ACRONYMS AND ABBREVIATIONS

AR	Aspect Ratio
CAD	Computer Aided Design
Cp	Power coefficient
Ct	Torque coefficient
HAWT	Horizontal axis wind turbine
OR	Overlap ratio
PLA	Polylactic acid
PVC	Polyvinyl chloride
Re	Reynold's Number
TSR	Tip Speed Ratio
VAWT	Vertical-axis Wind Turbine
CPVC	Chlorinated polyvinyl chloride

List of Tables

1 CHAPTER ONE: INTRODUCTION

1.1 Background

Today, wind turbines can generate even more energy to power water pumps than traditional windmills, which have been used to pump water for centuries.As a general rule, wind energy is used to pump water through a pump driven by a wind turbine. A wind turbine generates electricity, which is then used to power an electric motor to drive a water pump. An elevated or different location is then reached by pumping the water from a well, pond, or reservoir.An important advantage of using wind energy to pump water is its clean and renewable nature. Wind energy does not emit greenhouse gas emissions or air pollution, which makes it an environmentally friendly alternative to fossil fuels. Additionally, wind energy is abundant and free, which means that once the infrastructure is in place, it is relatively inexpensive to pump water using it. The ability of wind power to pump water in remote areas that are not connected to the electrical grid is another advantage of this method. In these areas, wind turbines can be used to power water pumps for irrigation, livestock watering, and other agricultural uses. In regions where water is scarce, this can improve the sustainability of agriculture and increase food production. Wind energy can, however, also be a challenge for pumping water. It is important to note that wind energy is intermittent, which means that the wind turbine may not always be able to generate enough electricity to power the water pump. It is possible that this will result in fluctuations in water supply, which can be problematic for agriculture and domestic use. In order to overcome this problem, some wind-powered water pumps are designed with energy storage systems that can store excess energy generated during periods of high wind and use it during periods of low wind.

1.1.1 Wind Turbine

Increasingly, renewable energy sources are being used to reduce the dependence on fossil fuels and to promote a more sustainable future. Wind turbines have become increasingly popular as a result. Wind energy is a clean and sustainable source of energy that does not emit harmful pollutants and greenhouse gases that contributes to climate change.Wind energy is one of the fast growing sources of electricity in the world ,with the global installed wind capacity reaching over 837 gigawatts(GW) in 2022(Global Wind Report,2022).
Wind turbines are devices that convert kinetic energy into electric and mechanical energy when the wind blows. They consist of rotor blades that turn whenever the wind blows.

Wind turbines are angled in such a way as to catch the wind and rotate the central shaft. The central shaft spins to generate the power. Wind turbines can be located either onshore or offshore. In contrast to a fan, a wind turbine produces electricity by using wind instead of electricity to create wind as does a fan. Wind turbines can be classified into two types: Vertical Axis Wind Turbine (VAWT) and Horizontal Axis Wind Turbine (HAWT).

1.1.2 Horizontal Axis Wind Turbine(HAWT)

Horizontal axis wind turbine is a type of wind turbine where the main rotor shaft is oriented horizontally and perpendicular to the direction of the wind.It is the popular choice for wind energy due to their proven technology and high performance.The blades of the turbine rotate around the axis,driven by the wind's force.
HAWTs are mainly used for electricity generation in wind farms,both onshore and offshore. They typically consists of three blades ,each of which is shaped like an airfoil to maximize its lift and generate power.
The main advantage of HAWTs is the ability to produce higher power outputs compared to Vertical axis wind turbines, with the higher efficiencies. But they have high maintenance cost,requires large amount of space and can be noisy.

1.1.3 Vertical Axis Wind Turbines(VAWT)

Vertical axis wind turbines are the types of wind turbines that rotate around a vertical shaft. They are applicable for small scale power generation, water pumping and for highway electricity generation.Vertical turbines can generate the power in any wind direction.They are also more complex to design and manufacture and have regular maintenance requirements. VAWT are viable option for wind generation in urban and limited spaces.
VAWTs have a advantage of quieter and require less wind to start rotating.They are also suitable for a wider range of wind directions, and their low profile design makes them easier for the installation in urban environments.
VAWTS can be classified into different types based on their design,including the Darrieus, Savonius and many more. The Darrieus types uses curved blades that resemble aerofoils,while the Savonius use the straight blades arranged around the vertical shaft.

1.1.4 Savonius Wind Turbine

Savonius turbines operate as drag type turbines.The Savonius turbines are excellent in areas of turbulent wind and are self-starting.Savonius turbines are easy to harvest the wind energy from lower speed to higher one as they are easy to transport in comparison to HAWT since HAWT are very large.The main principle of the Savonius wind turbine is that the drag coefficient on a concave surface is higher than that of a convex surface for having the same surface area(Oghoghorie, Ebunilo, & Orhorhoro, 2020). When the oncoming wind contacts the rotor, the concave side experiences a greater drag force than that of the convex side which causes the rotor to spin and the turbine rotates.
The Savonius wind turbines can be of different types based on the blade profiles. They can be of S-shape ,C-shape , L-shape ,Batch type and many more. Various researches have been done on the blade profile of Savonius wind turbines.Among them Helical Savonius wind turbines are found to be more efficient than the conventional straight blade Savonius wind turbine (Kamoji, Kedare, & Prabhu, 2009a).The Helical design makes the turbine to capture the wind from all direction.Helical Savonius perform at very low wind speeds making it more suitable for residential purposes.Helical Savonius is the promising technology with more environmentally-friendly option compared to other types of wind turbines.(Premkumar, Sivamani, Kirthees, Hariram, & Mohan, 2018)

Figure 1.1: Savonius turbine with Helical profile (Kumar et al., 2019)

1.1.5 Centrifugal Pumps

In a fluid system, a pump serves as a device that converts mechanical energy into pressure energy or kinetic energy, or both, of a fluid. A centrifugal pump transfers fluids by converting rotational kinetic energy into the hydrodynamic energy of the fluid flow. The fluid enters the pump impeller and is accelerated by the impeller, then flows out of the pump. They are of three types i.e i) Radial flow pumps (ii) Axial flow pumps (iii) Mixed flow pumps(Rajput, 1998)

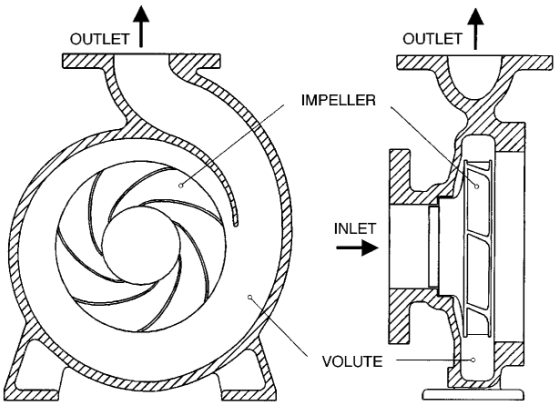

Figure 1.2: Drawing of Centrifugal Pump(Parrondo et al., 1998)

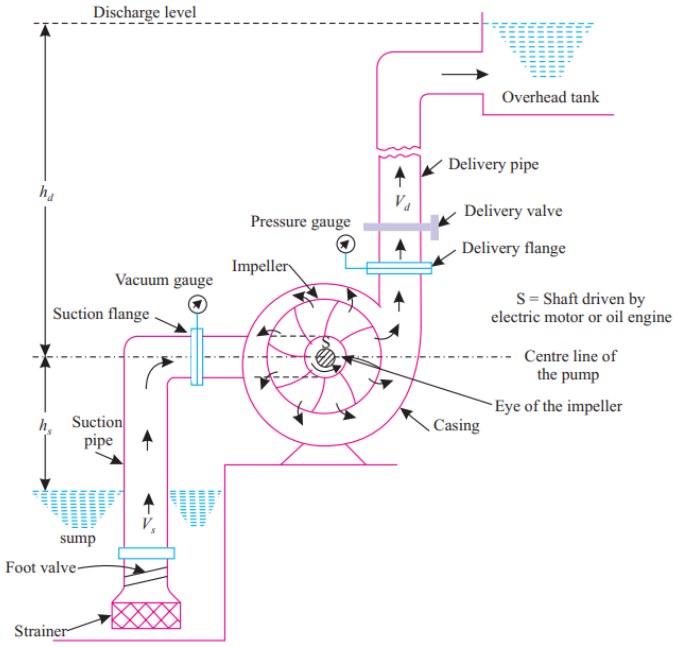

Figure 1.3: Centrifugal pump(volute type)–component parts. (Rajput, 1998)

1.1.6 Reciprocating Pumps

As a positive displacement pump, the reciprocating pump suctions and raises liquids by displacing it through a piston/plunger that is reciprocated within a cylinder that is closely fitting. Pumping an amount of liquid equals the volume displaced by the piston. There are two types of reciprocating pumps: single-acting pumps and double-acting pumps. The total efficiency of a reciprocating pump is approximately 10 to 20 % higher than that of a centrifugal pump of comparable size(Rajput, 1998).

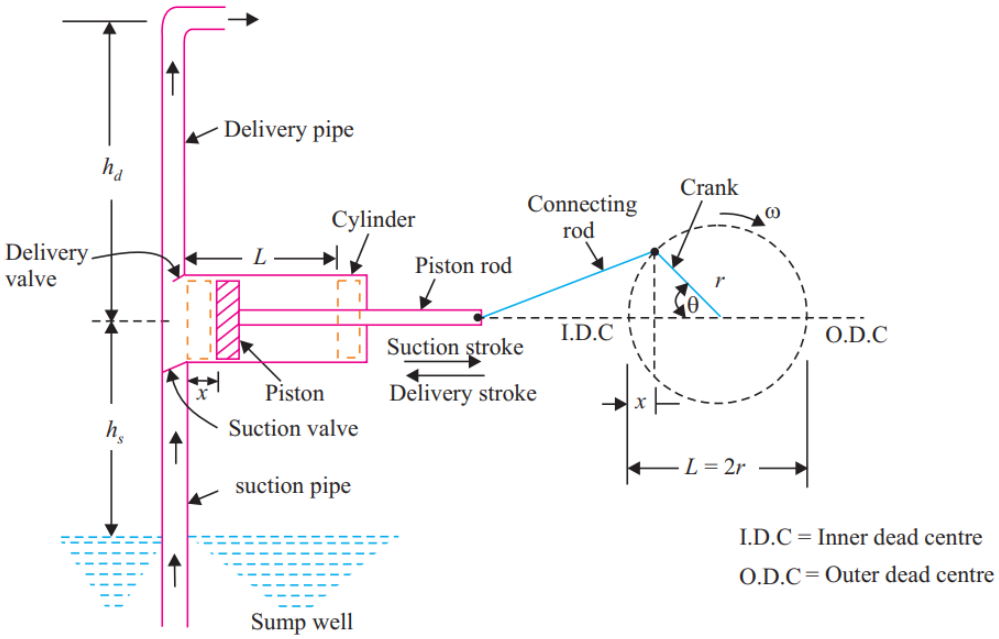

Figure 1.4: Schematic view of single-acting reciprocating pump(Rajput, 1998)

D = Cylinder diameter, m
A = Piston/cylinder cross-sectional area
r = Crank radius, m
N = Crank speed, r.p.m.
L = Stroke length (= 2r), m
h_s = Height to the centre of the cylinder from the liquid surface, m and
w = Liquid weight density N/m^3
h_d = Raised height to the liquid from the centre of the cylinder, m

$$\text{Driving power of Single-acting reciprocating pump } = \frac{wLAN * (h_s + h_d)}{60 * 1000}\text{kW} \quad (1.1)$$

$$\text{Driving power of double-acting reciprocating pump } == \frac{2wLAN * (h_s + h_d)}{60 * 1000}\text{kW} \quad (1.2)$$

1.1.7 Turbine Pump

Turbine pumps are centrifugal pumps that move fluids using rotating impellers. The impeller has curved blades that spin rapidly inside a volute casing, creating a centrifugal force that pushes the fluid towards the outside of the casing and out of the pump. The impeller in a turbine pump is usually made of bronze, stainless steel, or other materials that are resistant to corrosion and wear. The pump's motor is connected to the impeller through a shaft, which rotates the impeller at high speeds. Turbine pumps are commonly used in applications where high flow rates and low to moderate pressures are required. They are often used for agricultural irrigation, water supply systems, and in industrial applications where large volumes of fluid need to be moved.

1.1.8 Use of Vertical axis wind turbine in the field of water pumping

The vertical axis wind turbine (VAWT) can be used to pump water in areas where electricity is not readily available, or where grid connections are not feasible(Khammas, Hussein Suffer, Usubamatov, & Mustaffa, 2015). With VAWTs, blades rotate around a vertical axis instead of a horizontal axis as with horizontal axis wind turbines (HAWTs). Therefore, VAWTs are more suitable for environments with low wind speeds and changing wind directions. In areas where electricity is not readily available, or grid connections are not feasible, vertical axis wind turbines (VAWTs) can be used to pump water(Wadhai & Rangari, n.d.).

As a result of a central vertical shaft connecting several blades to the rotor, a VAWT is commonly known as a VAWT. In order to collect wind energy at higher altitudes, the rotor is generally mounted on a tall tower. VAWTs are used for pumping water from wells or other water sources to storage tanks or irrigation systems. Rotors are powered by gears or belt drives. In addition to being able to operate at low wind speeds, VAWTs are also effective at pumping water. Unlike HAWTs that require high wind speeds for electricity

generation, VAWTs can generate electricity when wind speeds are as low as 2-3 meters per second(Peimani, 2021). Due to this, they are suitable for use in areas that have low winds.

1.2 Problem statement

The Savonius turbine has a wide range of applications in the field of water pumping. A number of African countries where electricity is not readily available have utilized this technology to generate electricity. Since, Nepal is primarily an agricultural country with dry seasons throughout the winter, there is a difficulty with water for irrigation. Also, most of the places in Nepal do not have access to different types of pumping facility so, there has been pressing need to exploit the alternative energy. This problem could be solved if there were affordable pumps that was accessible to large numbers of people and that used alternative energy sources to operate.While wind speed feasibility study has been done in different locations of Nepal, there is gap in the research of potential of the Savonius wind turbine for pumping needs.So, this study aims to evaluate the suitability and efficiency of Savonius wind turbine for water pumping application.

1.3 Objectives

1.3.1 Main Objective

The main goal of the project is to design and fabricate the vertical axis savonius wind turbine and operate the water pump to study its efficiency.

1.3.2 Specific Objective

(a) To design and simulate the blade profile of Savonius wind turbine.

(b) To fabricate the helical profile of Savonius turbine.

(c) To compare the performance of Savonius turbine with the computational data.

(d) To study the performance of water pump powered by Savonius wind turbine.

2 CHAPTER TWO: LITERATURE REVIEW

2.1 Number of stages

An experiment conducted by Burton in 1988 revealed that the roto-dynamic pump outperformed the piston-displacement pump in terms of performance(Burton,1998). Ghosh, Kamoji,Kedare Prabhu,2009 found that the six peaks with a maximum static torque coefficient of 21% occurred at rotor angles ranging from 30 to 330 degrees. . At rotor angles of 45°, 105°, 165°, 225°, and 285°, the six troughs with the lowest static torque coefficient occur. Static torque coefficients does not depend upon the Reynolds number in the range studied. A single stage rotor system has better discharge than the multistage pumping system(Ghosh, Kamoji, Kedare, & Prabhu, 2009).

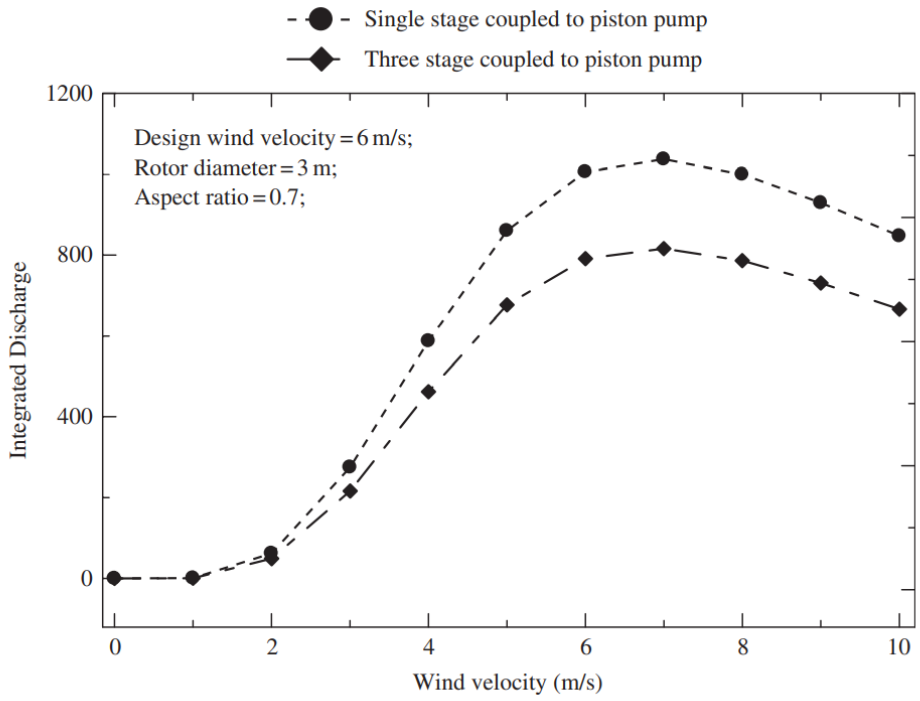

Figure 2.1: Change of discharge in m^3 /month with the wind velocity for single and three stage rotor which was coupled with the roto-dynamic pump (Ghosh et al., 2009)

2.2 Use of guide vane

In comparison with the Savonius turbine having no guide vane, the rotor having guide vanes generates significantly more power. Up to 65.69 % more power is generated(Salim

et al.,2019).

It has been found that Savonius wind turbines produce more power when the wind speed (v) increases. The addition of a guide vane increases the power coefficient when compared to wind turbines that do not have a guide vane. At 10.7 m/s, the Savonius wind turbine achieved 0.013 Cp. The maximum Cp of the Savonius wind turbine with the basic guide vane design is 0.018. The power increased by 27.66 percentage when compared to the maximum Cp of the rotor without a guide vane and with one. With the use of a rotor with a guide vane with a tilt of 45° in comparison with a rotor without a guide vane, the results improve by about 58.86 % and up to 65.90 % for the use of rotors with a guide vane with a tilt angle of 30°(Salim, Yahya, Danardono, & Himawanto, 2015).

2.3 Number of blades

In (Wijianti, Setiawan, et al., 2020), three profiles of wind turbines having 3 and 4 blades were tested using Savonius wind turbines. As a result of the tests, it is evident that the turbine with the number of blades 3 gives the best performance of the three profile models.In (Wijianti et al., 2020), three profiles of wind turbines with 3 and 4 blades were tested using Savonius wind turbines(Wenehenubun, Saputra, & Sutanto, 2015).

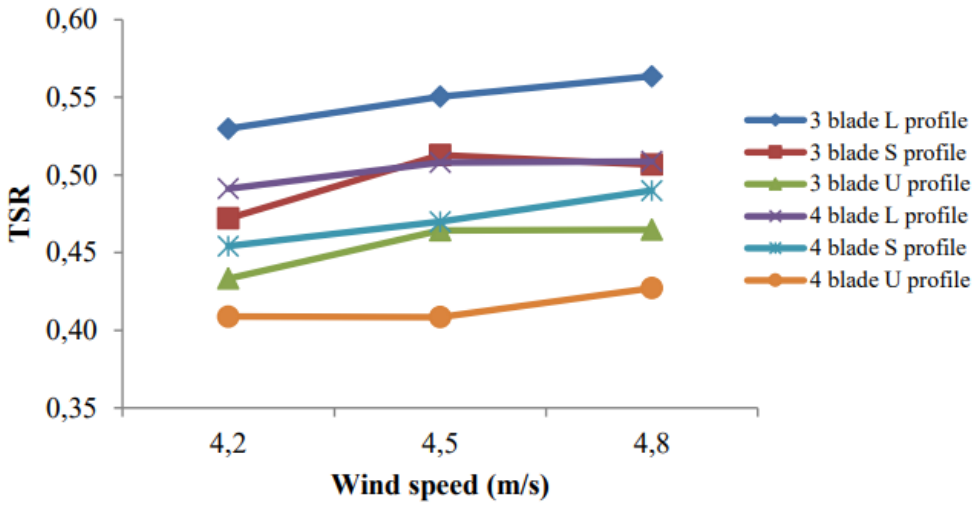

Figure 2.2: Wind Speed Vs TSR (Wijianti et al., 2020)

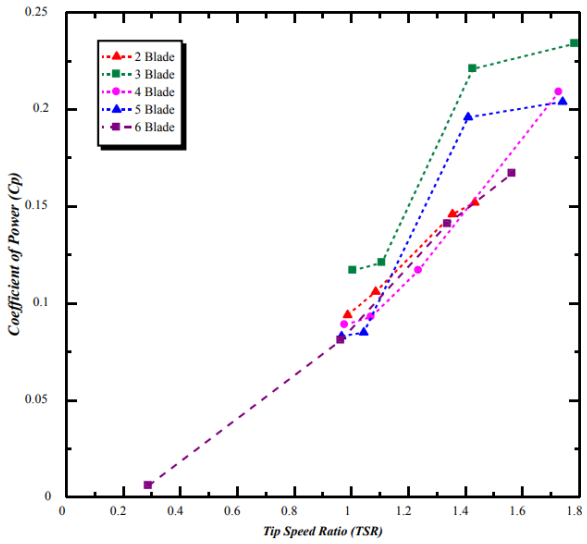

Figure 2.3: Tip Speed Ratio Vs Coefficient of performance. (Hamzah et al., 2018)

2.4 Design of blade

In the research it was found that the lift and drag coefficient was increased by 65% by the use of Novel Blade at certain optimal angle. It is a measure of the imbalance of forces on both sides of the advancing blade and the returning blade, which is the difference between the total drag force on the concave contour and the lift force on the convex contour. The disparity of the Novel Blade was reduced by 93 % (0.0065 versus 0.0824) when compared to that of the Savonius type, indicating that the Novel Blade improves the aerodynamic performance of the rotor and minimizes oscillation and noise(Chang, Tsai, & Chen, 2021).

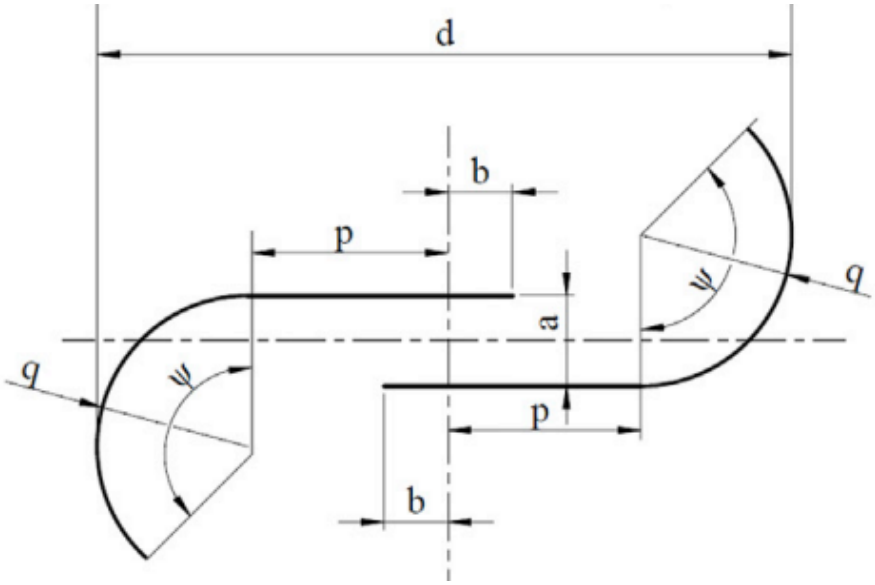

Figure 2.4: Schematic Drawing of Blade profile(Damak et al., 2018)

2.5 S-Rotor Savonius Wind Turbine

For the S-rotor, different Aspect Ratio and Overlap Ratio values have been observed in the optimization study. From the S-rotor, the highest yield was obtained with Overlap Ratio and Aspect Ratio values of 0.068 and 0.848 respectively(YİĞİT, 2020).
A positive effect of opening the overlap distance to the center of the S-rotor was observed on its performance. As the air passes through the overlap distance, it assists the rotor in rotating by hitting the center of the S-rotor. Increasing the overlap distance to the center of the rotor greatly improves the performance of the S-rotor.

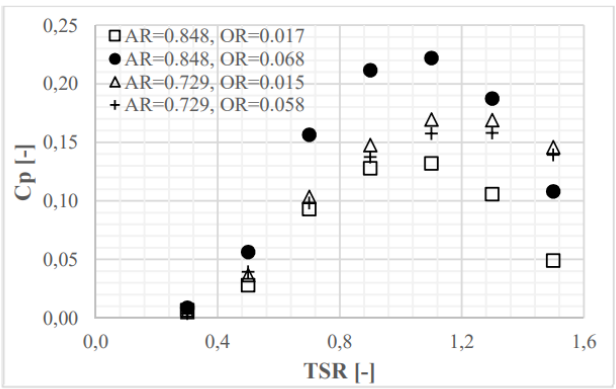

Figure 2.5: Variation of C_p to TSR for various Design of Experiment. (YİĞİT, 2020)

2.6 Helical Savonius rotors

The Helical Savonius rotor has a high performance due to the fact that the aspect ratio is 0.88, which makes it performance superior to rotors that have aspect ratios of 0.93 and 1.17(Kamoji, Kedare, & Prabhu, 2009b). This is due to the fact that the rotor's performance is highly dependent upon the Reynolds number. As Reynolds number increases, the maximum coefficient of power of the rotor will also increase. For a helical Savonius rotor with aspect ratio of 0.26, the correlation equation for a helical Savonius rotor will look as follows: The overlap ratio for Reynolds number 88 is zero, and the ratio for Reynolds number 88 is 0.88 numbers ranging from 86,600 to 202,000. The static torque coefficients at all the rotor angles for all helical rotor was positive. But in the case of conventional Savonius rotor, there are several rotor angles at which static torque coefficient is negative(Kamoji et al., 2009b).

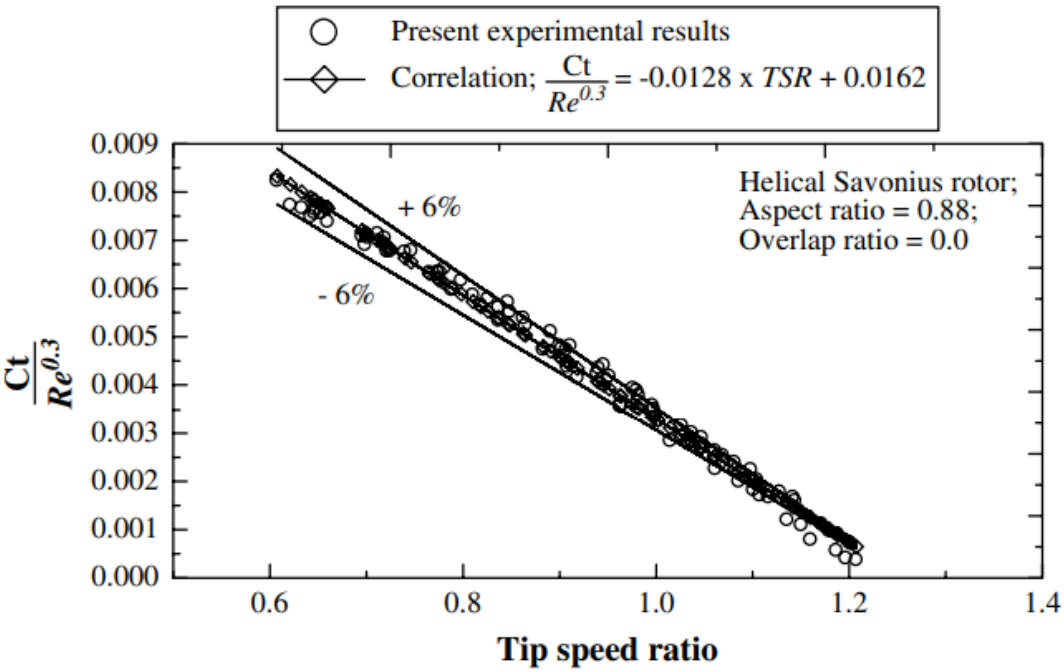

Figure 2.6: Reynolds numbers (from 86,600 to 202,000) variation effects on helical Savonius rotor (Kamoji et al., 2009b)

2.7 Numerical modelling and design of Vertical Axis Helical Wind Turbine

According to the CFD analysis, the coefficient of performance for a variety of aspect ratios has been determined, with the coefficient of power being 0.3927 for the rotor with an aspect ratio of 1. On the basis of both power generation and efficiency, this turbine has been considered to be the most economically efficient turbine around. A vertical axis helical wind turbine with an aspect ratio of 1 can serve as a valuable renewable energy source for highways as a valuable renewable energy resource. By using impact wind energy, which is generated by moving vehicles on the highways to generate electricity that can be stored in batteries and then used in a variety of ways, including traffic signals and street lights, we can generate electricity that is able to be used for a variety of purposes. The results from the experiment indicate that impact wind energy at 4 pm has a velocity of 7.86 meters per second, which is a velocity that generates a maximum power of approximately 3.46 watts with the help of the prototype running at a speed of 446 rpm(Bartaula & Shakya, 2020).

2.8 Helical Savonius rotor optimization through wind tunnel experiments

A novel vertical wind turbine based on helical Bach rotors has been presented by (Damak et al., 2018) in the form of a helical Bach rotor. A hybrid of a Bach rotor and a helical rotor, the Bach rotor, had a high power coefficient Cp, but a negative static torque coefficient, which made it impossible for it to start on its own at certain angles due to the negative static torque coefficient. As well, helical rotors were also known to have lower power coefficients than Bach rotors, but also to have a positive static torque coefficient. In order to accomplish this, this research designed a new rotor using resin and glass fiber and tested it in the wind tunnel. This rotor would be combined to produce an improved helical Bach rotor. In order to determine the power, torque, and static torque coefficients of each rotor, the following test methods were used. As compared to helical rotors, helical Bach rotors have the highest power coefficients and static torque coefficients, according to experimental results. A power coefficient of approximately 0.2 was found for the helical Bach rotor, whereas a power coefficient of approximately 0.18 was found for the helical rotor for the helical rotor.

2.9 Study on performance improvement of twisted-bladed Savonius wind turbines

The literature (Saad, El-Sharkawy, Ookawara, & Ahmed, 2020) explains that the design parameters like the twist angle, overlap ratio, and end plate sizes along with wind velocity affect the overall performance of the turbine. For the analysis RANS k-w model was developed. Compared to other models of turbines, the Savonius turbine with a 45-degree twist angle achieves the highest output power. Increasing the overlap ratio in the turbine causes the formation of eddies and the loss of kinetic energy. A maximum power coefficient of 0.174 was found to be the maximum power coefficient(Saad et al., 2020).At some rotor angles, it was also observed to be negative static torque.

2.10 Design of a Vertical Axis Wind Turbine Operated Water Pump

(Oghoghorie et al., 2020) researched about the designing of the optimum functioning system of the Savonius turbine which was operated by the pump was done.The diameter of the turbine blade was 1.45m and the length was 2.35m. The test was performed on the wind velocity of average 3.49 m/s on the turbine of swept area of 3.41m^2.Thus, from the analysis the flow rate of 47.77liters of water per 3.08 minutes was operated where the average value of flow rate was 16.16 liter per minute.So the performance of the Savonius turbine with the pump operation was found satisfactory in Nigeria.

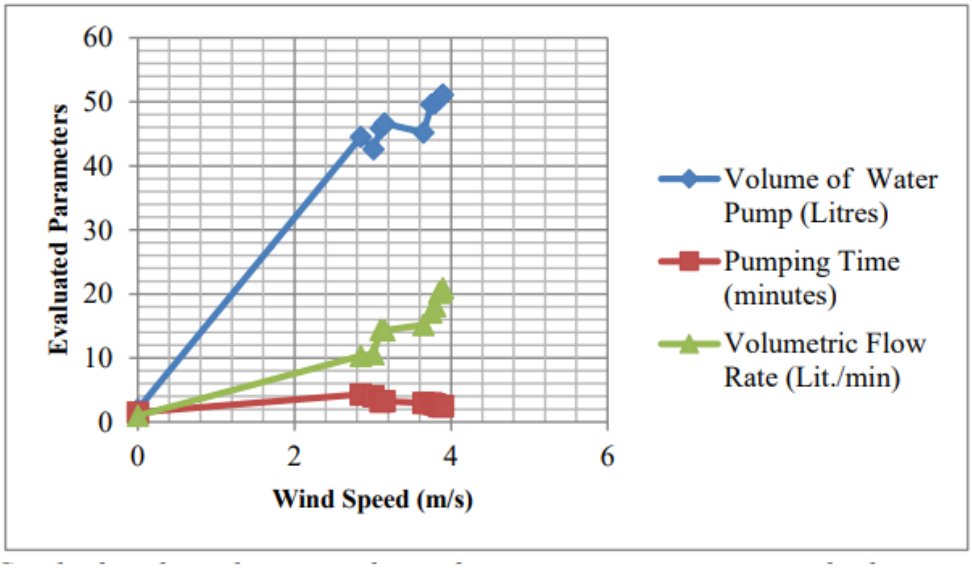

Figure 2.7: Relation of wind speed with pumping time, volume of water pump and volumetric flow rate.(Oghoghorie et al., 2020)

2.11 Wind powered water pump design for irrigation

(Permadi, Andari, Sapsal, et al., 2019) developed a model of a pump utilizing a vertical axis Savonius wind turbine. The test was conducted at a average wind speed of 3.6 m/s with a rotational speed of 5.6 rpm. After analyzing all the data obtained, the average flow rate of 2.03 liters of water per minute was calculated with an efficiency of 0.897. It was found that the discharge of the pump varies in accordance with the number of rotations of the windmill and the speed of the wind.

N°	Windmill Spin (Rpm)	Wind Velocity (m/s)	Water Volume(cm^3)
1	4.00	2.37	1285.56
2	4.83	3.11	1879.17
3	5.08	3.34	1733.33
4	5.13	3.11	1896.25
5	5.44	3.38	2005.56
6	6.22	2.98	2311.11
7	6.27	4.79	2263.64
8	6.33	4.77	2266.67
9	7.08	4.15	2670.83
Average	5.6	3.6	2034.7

Figure 2.8: Variation of windmill rotation, wind speed, and the flow rate of water (Permadi et al., 2019)

2.12 Study on coupling of roto-dynamic Pump and savonius Wind Turbine for wind energy water pump system

A study by (Lukiyanto, 2016) examined the Savonius windmill, measuring 1 m in height and the diameter of 0.8m , with two buckets and a centrifugal pump in two stages. By replacing a couple of fixed orifices and sliding orifices with a double U pipe configuration, the pump was viable for the low speed shaft of the system. Several belts and pulleys were used to transmit the shaft of the windmill into the pump. As far as a 1.5m head is concerned, the shaft speed is 120 rpm, with a shaft power of 13 watts, and the cut-in speed is 4.5 m/s for the 1.5m head. As observed during the observation, the wind speed matched the shaft speed to the cut-in speed such that the turbine was able to operate effectively, and the transmission ratio was found to be adequate(Zemamou, Aggour, & Toumi, 2017).

2.13 Characteristics of wind turbine operated Reciprocating Piston Pump

The research by (Kedare & Date, 1990) was based on the starting torque of reciprocating piston pumps. The pumps that are operated by wind machines have very high starting torques, which adversely affect the starting speed. As the starting torque decreases, the piston pump by which the wind machine operates will become faster, decreasing the operating time for the turbine. As a result of this method, the pump stroke volume can be adjusted or the flow rate can be adjusted. Therefore, these two methods can be applied by drilling a small hole which lowers the piston pressure, resulting in a low starting torque, but there will be a greater possibility of water leakage in this case. It was observed in this study that the discharge of the normal pump is higher, but the cavitation phenomena will be less, which ultimately improves the performance of the piston pump.

2.14 Water Pumping System fabrication by Using Vertical Axis Wind Mill

The article by (Vignesh, Christopher, Albert, Selvan, & Sunil, 2020) researched on the windmill which can be used in remote places where electricity is not available for agricultural purposes. The wind energy obtained can be directly used to operate pumps. Here, a multi-blade wind turbine with a piston pump was used where the windmill was attached to the piston pump through the discs. The rotation of the windmill is converted into the reciprocating motion of the pump. The paper also recommends that various parameters for the windmill design must be considered for the advantage of this type of project.

2.15 Design and Fabrication of wind turbine powered reciprocating water pumping system

The project by (Nayeem, Kumar, Bhaskar, Jnanendra, & Kumar, 2019) is about the windmill and the pumping. The up-down motion of the handle is given to the piston where the water is sucked using the difference in pressure from the lower ground. The pump used was the reciprocating water pump which was incorporated by the check valves that allowed the water to flow in the upper direction. A torque of 106.4572 Nm was obtained with a flow rate of 0.1736 liters per second. The total number of blades used was 24 with a surface area of 0.5585 $m2^2$.

2.16 Vertical Axis Wind Turbine to Power a Well Pump

This project (Rusenko, Hontz, Zhang, Norton, & Erdman, 2014) aims to investigate sustainable methods of powering mechanical well pumps in developing societies in a social and environmental manner. In this case, the vertical axis used was a conjunction of Savonius and Darrieus. The turbine was tested in the Penn State wind tunnel at a speed of 26.1 feet per second. Power was extracted from the turbine through the use of a DC motor connected to the turbine directly with a shaft that rotated. In general, the increase in wind speed increases the voltage generated. Although the expected results were not achieved, the researchers have recommended improving the shape of the airfoil and using deflectors to change the direction of the wind. The speed of rotation of 66 rpm was observed at a wind speed of 20 ft/s.

2.17 Vertical-Axis savonius wind turbine optimization for Water pumping application in rural Africa

As described in (Zingman, 2007), the thesis aims to improve the current water pump operated by the wind system which was produced by D-lab Honduras. The developed Savonius rotor was turned on from 70 RPM to 100 RPM with significant torque before connecting the pump. The Savonius rotor was tested in the Toyota Celica convertible with the addition of the 'wind tunnel' system at a speed of 15 mph. The washer and rope pump was used in conjunction with the drive train. In this study, the Savonius rotor performance was found to be less than ideal. In the thesis, the researcher proposes measures to reduce weight and friction, thereby allowing the Savonius rotor to power rope and washer pumps independently by reducing friction load. In addition to friction load, torque decreased with increase in speed without consideration of bearing friction.

3 CHAPTER THREE: METHODOLOGY

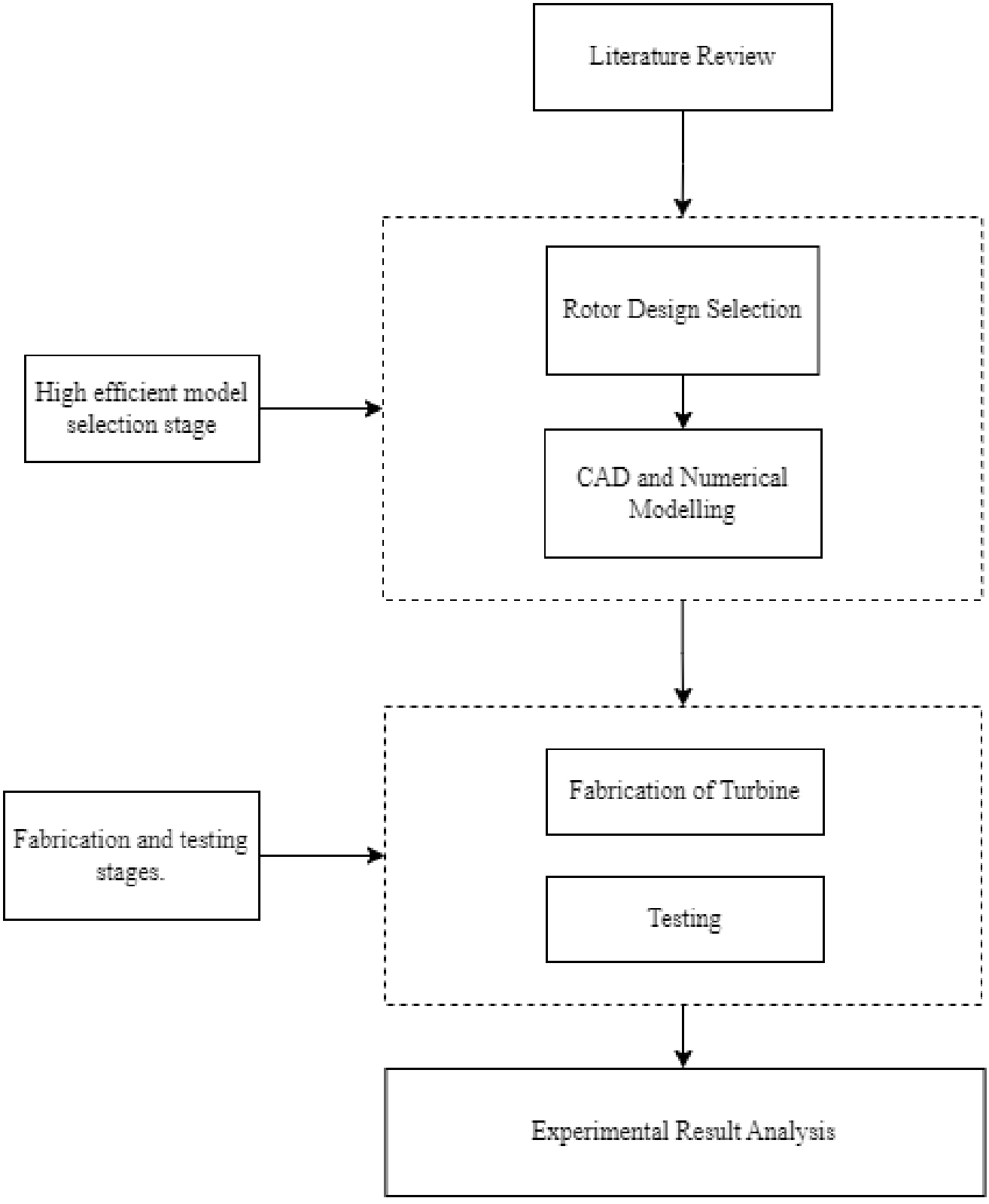

Figure 3.1: Process Flowchart

3.1 Workflow

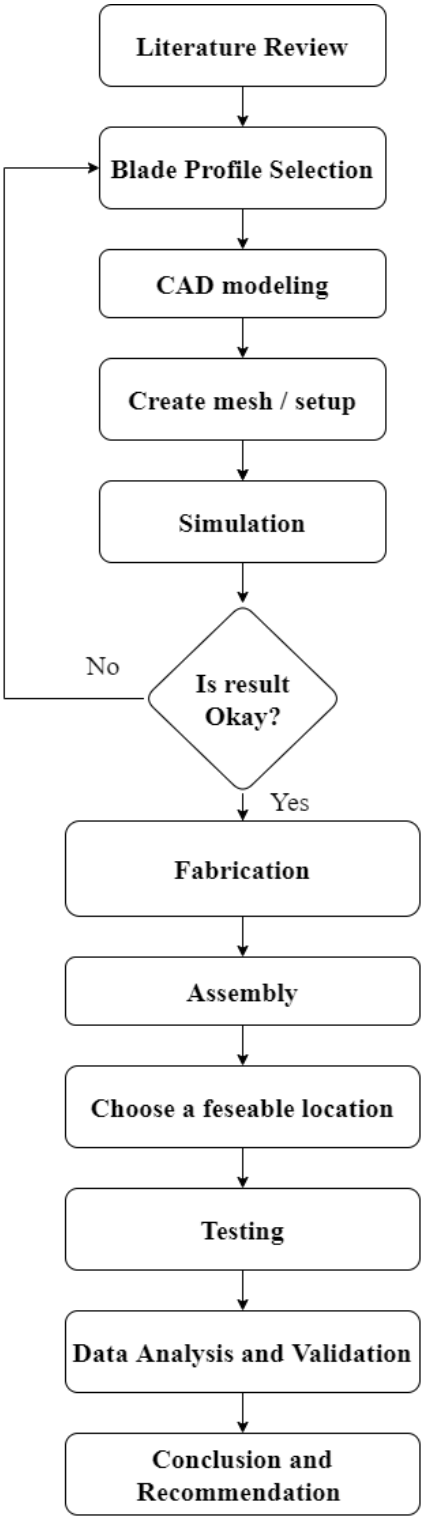

Figure 3.2: Work Flowchart

3.2 Literature Review

Initially,numbers of research paper were studied to determine the responsible factor affecting the performance of the helical savonius turbine. Geometrical parameter of the rotor design for the highest efficiency of the batch type savonius turbine was selected and similar research that were done previously in different countries were studied for the basis of completion of this project.

3.3 Design

Based on the literature reviews of the various articles and researches,the best blade design for Helical Savonius was selected. It was found that the helical Bach rotor had the highest power coefficient and torque coefficient(static) compared to the other helical rotor. The helical Bach rotor had a power coefficient of 0.2, whereas the helical rotor had a power coefficient of 0.18.(Damak et al., 2018) After considering all the design parameters for the rotor, 3D modeling was carried out in SolidWorks.

3.3.1 Numerical Formulation

It is possible to calculate the torque coefficient (Ct) and power coefficient (Cp) through the following equation .

Power coefficient of rotor is expressed as,

$$C_P = \frac{P_{rotor}}{P_{max}} \tag{3.1}$$

Power of Savonius rotor P_{rotor} is expressed as,

$$P_{rotor} = \frac{1}{2}\rho A({V_1}^2 - {V_2}^2)R\omega \tag{3.2}$$

Formula to extract maximum power P_{max} from wind is given by,

$$P_{max} = \frac{1}{2}\rho A {V_{freeblock}}^3 \tag{3.3}$$

Power coefficient is calculated as follows,

(3.4)

$$C_P = \frac{\frac{1}{2}\rho A(V_1{}^2 - V_2{}^2)R\omega}{\frac{1}{2}\rho A V_{\text{freeblock}}{}^3}$$

Tip speed ratio of the Savonius wind rotor is

(3.5)

$$\lambda = \frac{u}{V} = \frac{\pi DN}{60V} = \frac{R\omega}{V}$$

The torque co-efficient of the Savonius rotor is calculated as,

(3.6)

$$C_t = \frac{C_p}{\lambda}$$

VAWT swept area depends on both the diameter and blade length of the turbine, so

(3.7)

Swept area(A_s) = $D_t l_b$

where,
A_s = Savonius wind turbine swept Area (m^2)
D_t = Turbine diameter (m)
l_b = Turbine blades length (m)
As power of the wind is directly proportional to the density of the air, as well as the area of the segment of the wind .The relationship between density,wind speed and area of the segment of wind is expressed mathematically as.

(3.8)

$$P_w = \frac{1}{2}\rho A V^3 C_{Pmax}$$

where,
P_w = Power of the wind (watts).
ρ= Density of air (1.293 kg/ m^3).
A= Area of a segment of the wind being considered (m^2)
V = Wind speed (m/sec)
C_{Pmax} = Power coefficient

Hence the difference between output power and the input in the wind gives the extracted mechanical power which is given as
$P_{m,ideal} = \frac{1}{2}\rho\left(\frac{16}{27}AV^3\right)$

Betz coefficient = $\frac{16}{27}$ = 0.593 which indicates that actual turbine cannot extract more than 59.3 percent of the power.
Tip speed of blade is calculated from the length of the turbine blades and the rotational speed of the turbine

(3.9)

$$\text{Tip Speed of blades} = \frac{Rotational speed(rpm) \times \pi \times D}{60}$$

Where, T is Torque (N-m), ρ is density of wind (kg/m^3), V is wind velocity (m/s), A is the cross-sectional area (m^2), N is rotor speed (rpm) and ω is the angular velocity (rev/sec) and D is overall rotor diameter (m)

3.3.2 Rotor Design

The design parameters for the Helical Savonius rotor were specified and the selection blade profile was done.Using the design parameters, an initial blade shape was determined and the performance are to be determined considering the factors like power,torque and ease for the operation of pump.

3.3.2.1 Determining the Basic Design Parameters The aspect ratio and rotor height of the Helical Savonius rotor was specified.The radius of the rotor was estimated from the equation:
Aspect Ratio (AR) = $\frac{\text{Height}}{\text{Diameter}}$

Gap size effects on peak power coefficient
Gap size (a/d)= 0
where, a=blade gap size and d= rotor diameter

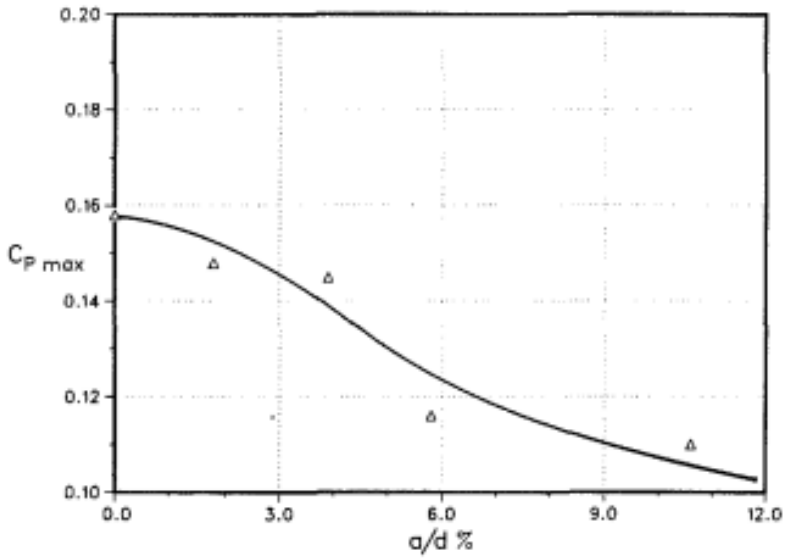

Figure 3.3: Gap Size effects on Peak Power Coefficient
(Modi & Fernando, 1989)

Overlap ratio effects

Blade overlap ratio(b/d)= 0

where, b=blade overlap and d=diameter of rotor

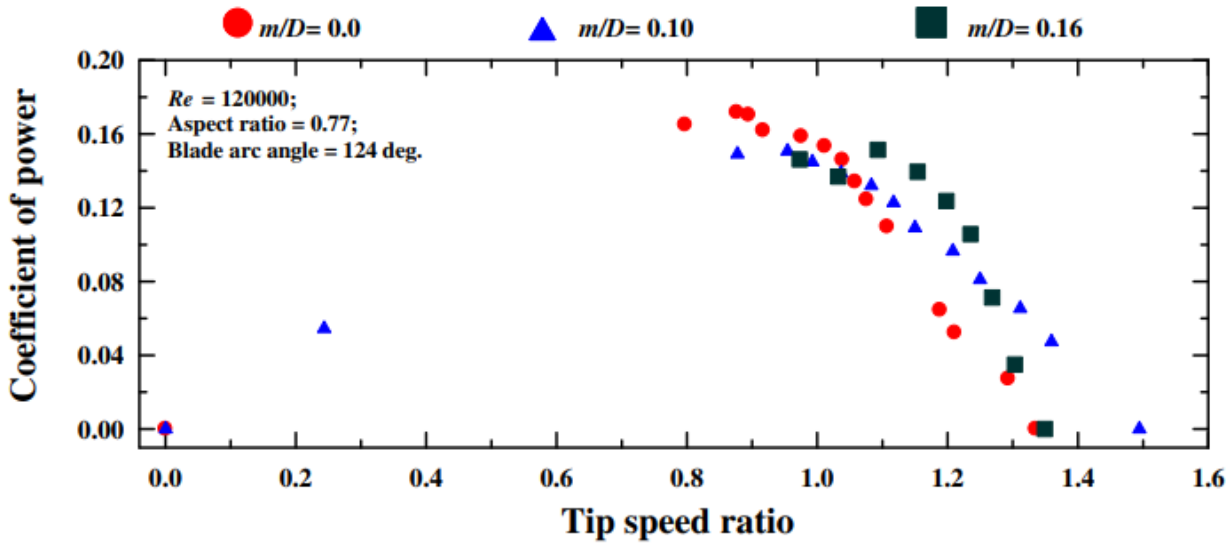

Figure 3.4: Overlap ratio effects on coefficient of power
(Kamoji et al., 2009a)

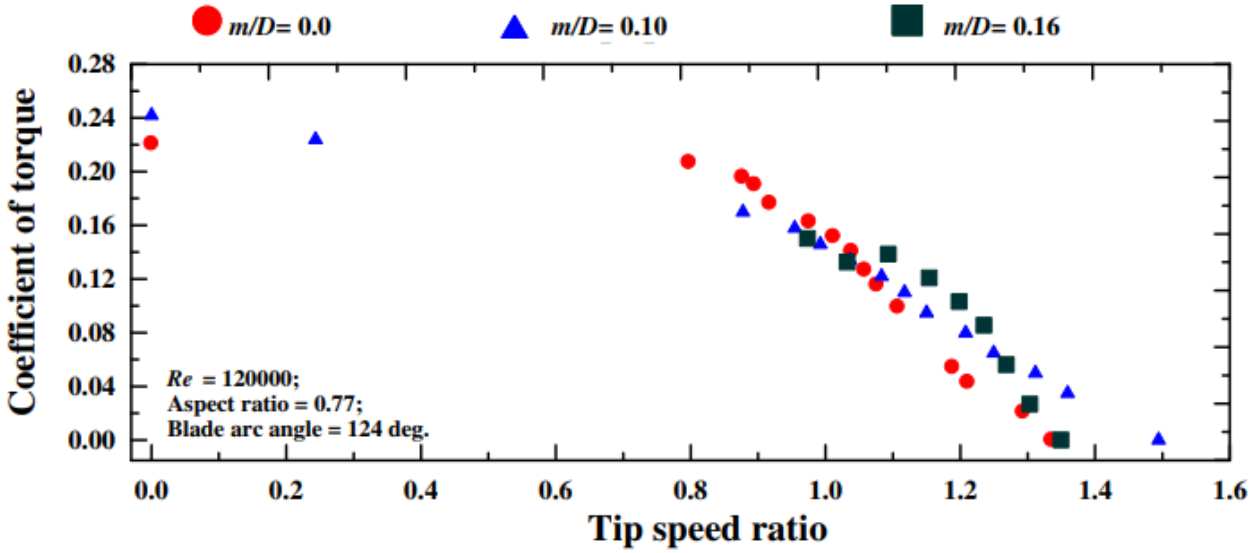

Figure 3.5: Overlap ratio effects on coefficient of torque
(Kamoji et al., 2009a)

Aspect ratio effects

Aspect ratio (AR)= 0.7

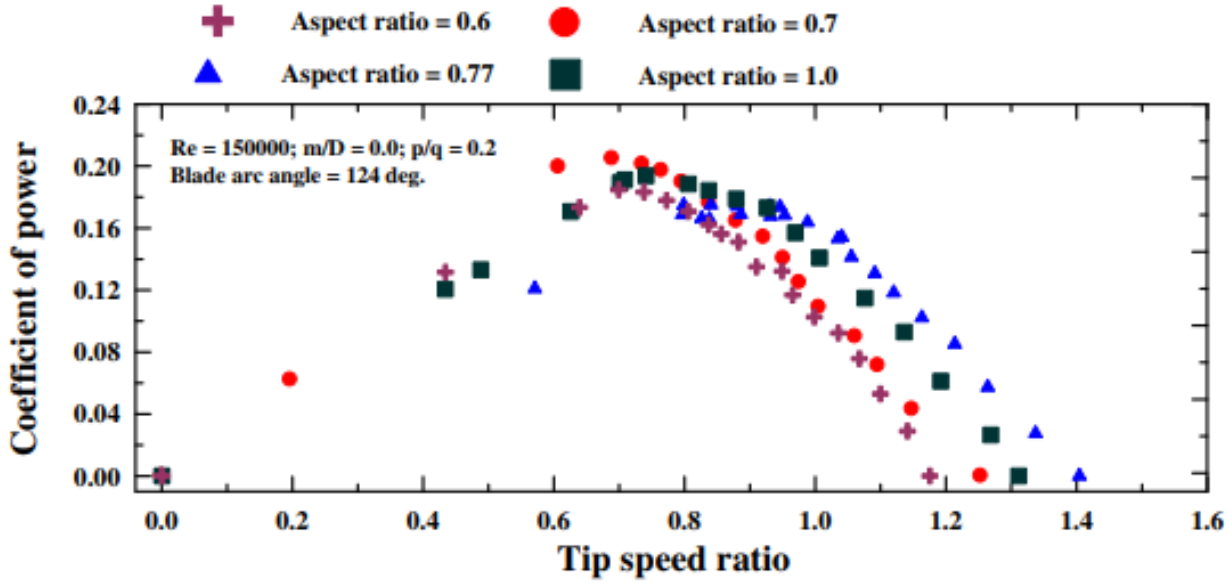

Figure 3.6: Aspect ratio effects on coefficient of power
(Kamoji et al., 2009a)

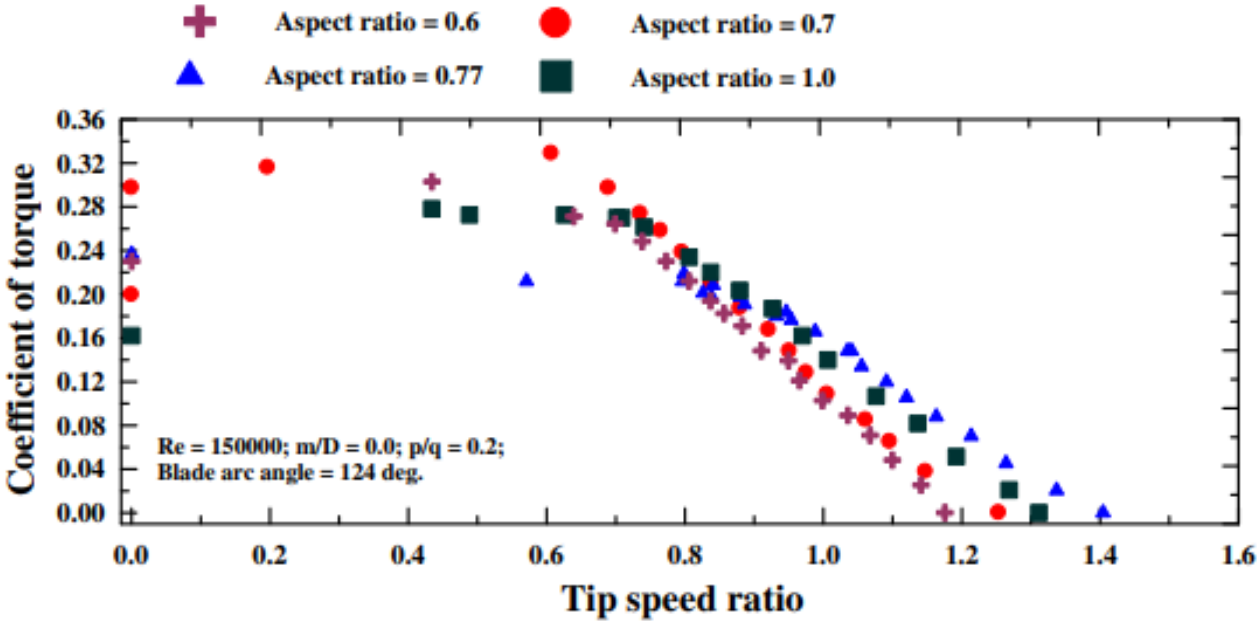

Figure 3.7: Aspect ratio effects on coefficient of torque
(Kamoji et al., 2009a)

Blade shape parameters effects

Blade shape parameters(p/q)= 0.2

where, p=length of straight edge of blade and q= radius of circular arc

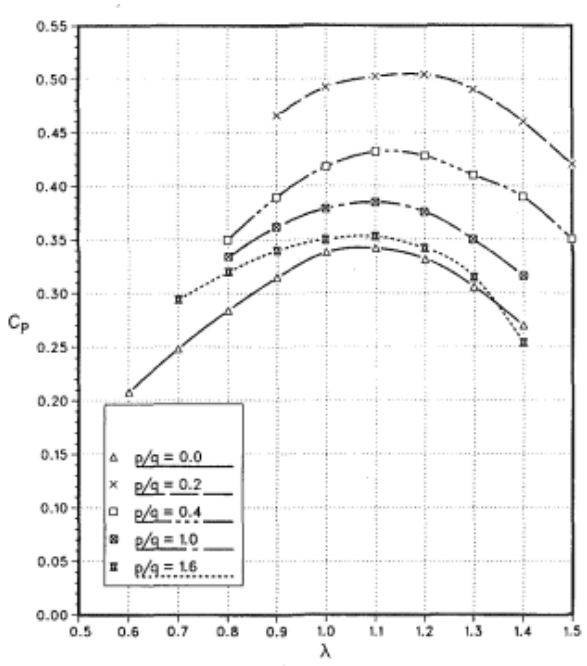

Figure 3.8: Blade shape parameters effects on the power coefficient (Modi & Fernando, 1989)

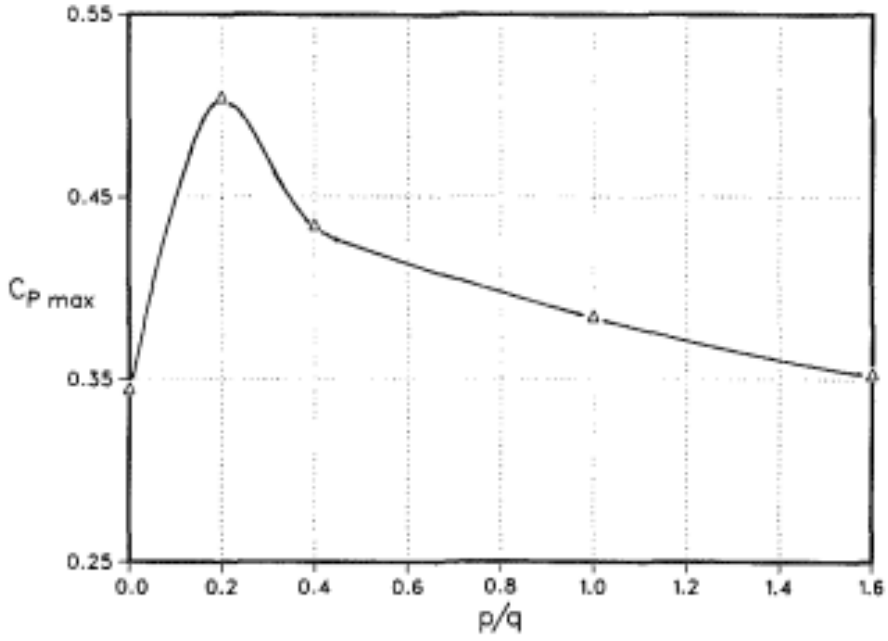

Figure 3.9: Peak power coefficient variation with Blade shape parameters (Modi & Fernando, 1989)

Blade arc angle effects

Blade arc angle (ω)= 124°

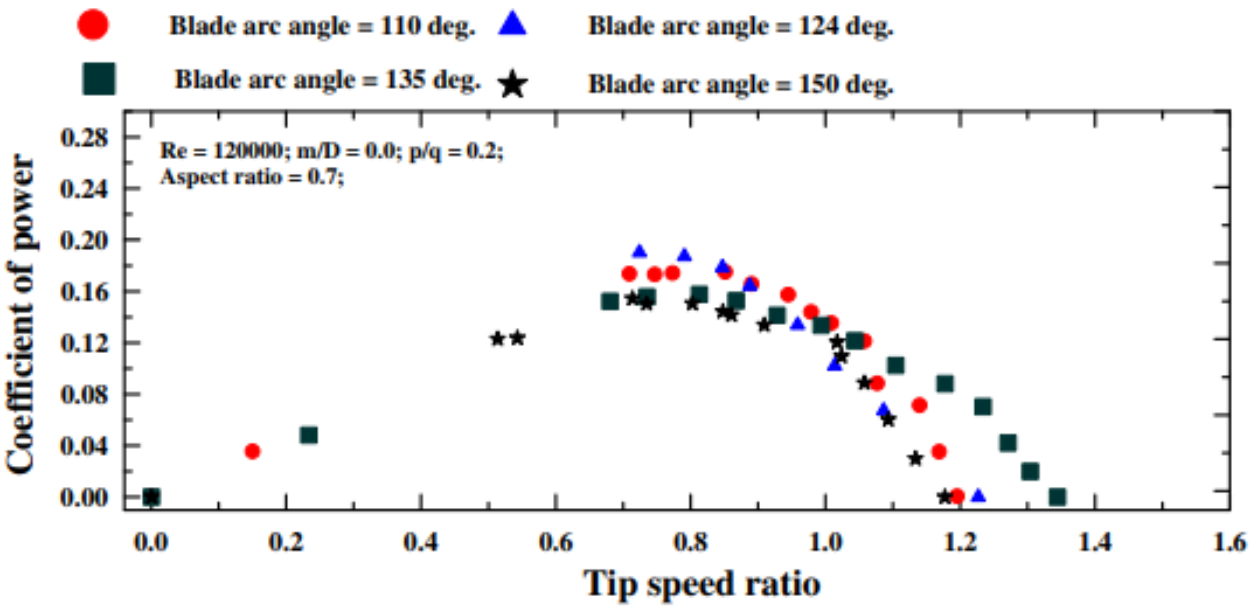

Figure 3.10: Blade arc angle effects on coefficient of power
(Kamoji et al., 2009a)

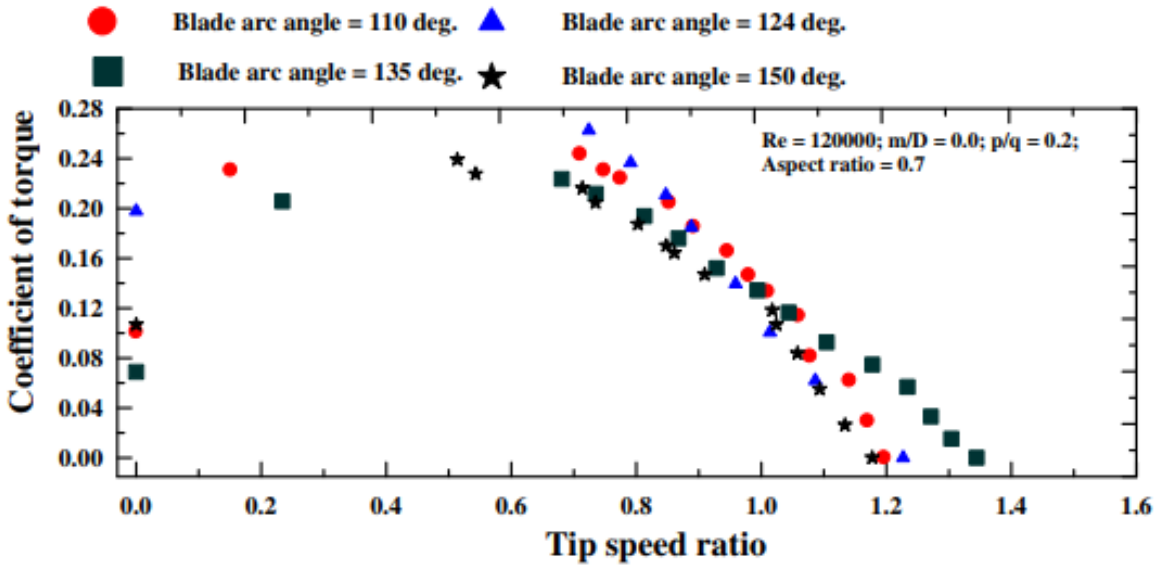

Figure 3.11: Blade arc angle effects on coefficient of torque
(Kamoji et al., 2009a)

In summary, the design parameters are listed on the table below:

Geometric Parameters	Value
Aspect Ratio	0.7(Zemamou et al., 2017)
Rotor Height	0.7m
Rotor Diameter	1m
Overlap ratio	0 (Kamoji et al., 2009b)
Number of Blades	2 (Wenehenubun et al., 2015)
Blade arc angle	124°(Kamoji et al., 2009a)
Twist angle	90°(Damak et al., 2018)

Table 3.1: Design Parameters

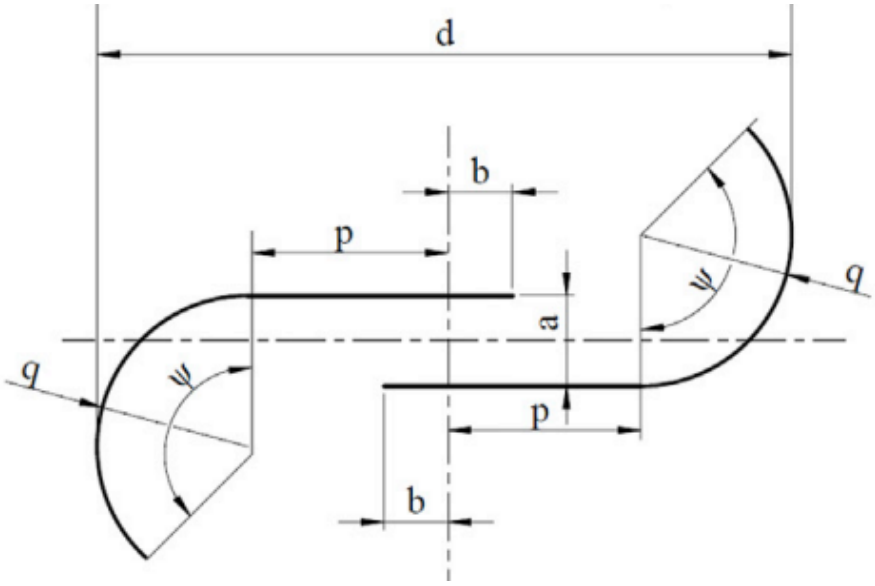

Figure 3.12: Schematic Drawing of Blade profile(Damak et al., 2018)

3.3.3 3D modeling

After the blade profile was selected the modeling of the rotor was done in SolidWorks 2021. The isometric view of the blade profile is as shown below.

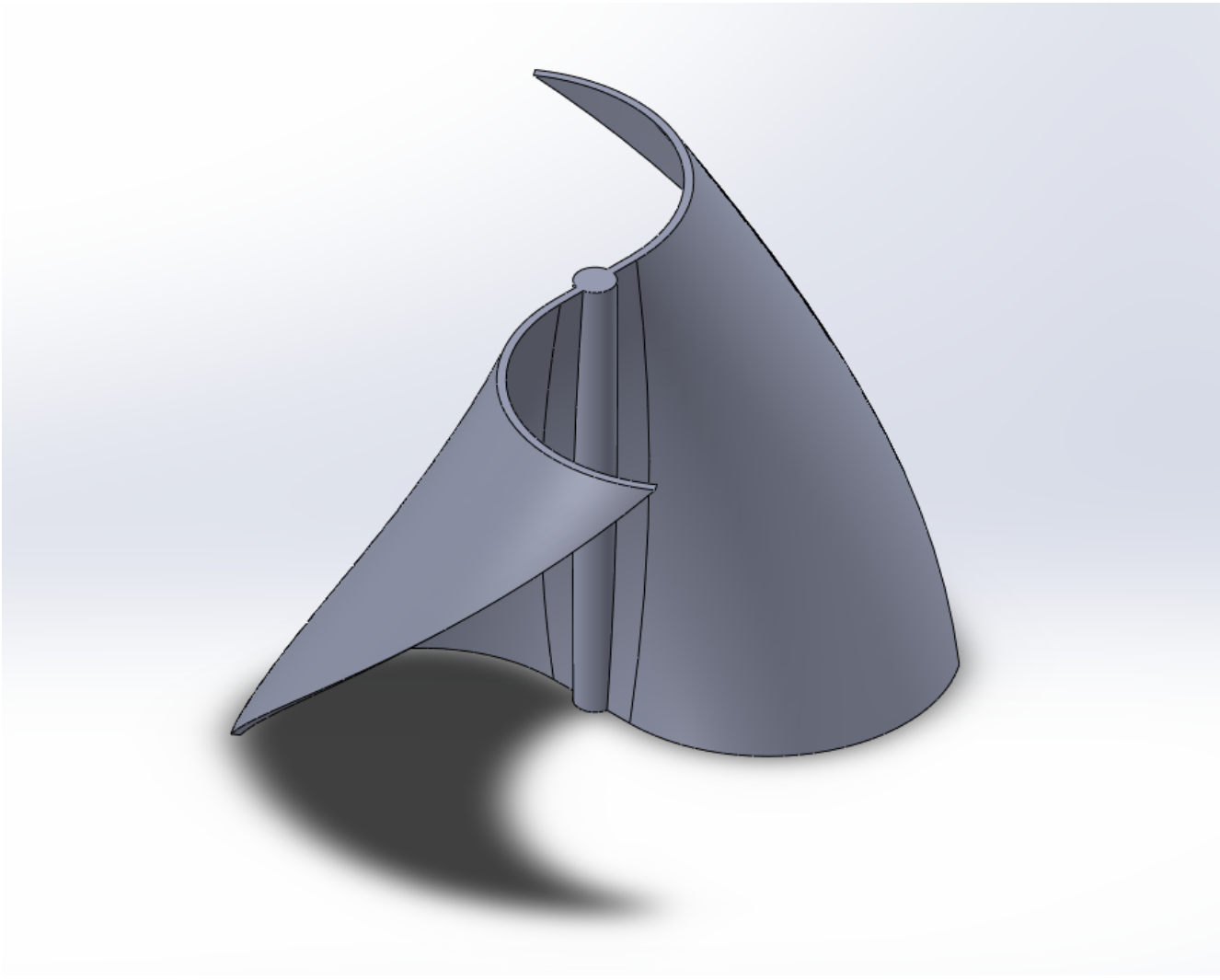

Figure 3.13: Isometric View

3.3.4 Design of Shaft

The design of shaft must be done according to the rotational torque that the rotor imparts to the shaft. The design is based on the considerations and literature reviews.

Some assumptions were done before the design are as follows:
Considering the maximum velocity = 10 m/s
Factor of Safety(FOS)= 7
Maximum rotational speed = 200rpm

Based on the assumptions above, the power is calculated as Power(P)= $\frac{1}{2}\rho A v^3$ =452.55 W

The ultimate strength of sheet metal that was used in the turbine was 49.4 MPa.

P = $\frac{2\pi NT}{60}$
$\Rightarrow$ T= 21.60 Nm

We know,
T $\times FOS = \frac{\pi}{16} \times d^3 \times \tau$

Solving, we get
d=24.98mm

Nearest standard size available in the market was 25.4 mm shaft.
So, the shaft of 1 inch diameter was selected.

Though maximum velocity is assumed to be 10m/s the operating velocity is found to be with an average velocity of 4m/s so,power extraction calculation is done with the average velocity of 4m/s (Laudari, Sapkota, & Banskota, 2018)
With the average wind velocity = 4 m/s
Factor of Safety(FOS)= 7
Based on the assumptions above,
Possible energy that can be harvested with average wind velocity of 4m/s is
Power (P) $= \frac{1}{2}\rho A v^3 = 28.96\,\text{W}$

3.3.5 Design of Rotor

For a model turbine
Number of blades N = 2
Density of air = 1.293 kg/m^3
C_p = 0.2 (Goh & Schlüter, 2016)
Average wind velocity(V) = 4 m/s

Expected Power = 6 W
Theoretical Power (P_w) = $\frac{6}{0.2}$ W = 30 W,
Aspect Ratio(AR) = 0.7
H = 0.7D
So,
Power (P) = $\frac{1}{2}\rho A v^3$
$30 = \frac{1}{2} \times 1.293 \times (0.7D \times D) \times 4^3$ $\quad [A = H \times D = 0.7D \times D]$
Solving, we get
D = 1m
$H = 0.7 \times D = 0.7\,\text{m}$

3.4 CFD Analysis

3.4.1 Fluid Flow Domain Formulation

For the formation of the fluid domain, it should be large enough to capture the flow pattern around the turbine, as well as extend upstream and downstream of the turbine. Therefore, for appropriate analysis, the overall domain was divided into two zones. The domain is divided into two sub-domains: the surrounding fixed blades and the inner rotating blades A rectangular fluid domain was created using the design modeler. The enclosure feature was used to define the fluid domain. Booleans were created to subtract the turbine from the rectangular fluid domain, whose boundaries were referred to as inlet, outlet, walls, rotor, rotating domain, and stationary domain.

3.4.2 Meshing

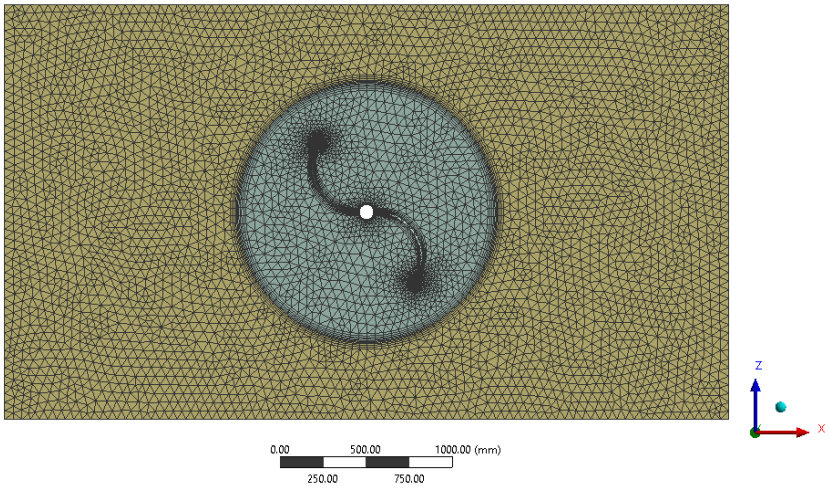

Figure 3.14: Three-dimensional Internal Region of the Computational Mesh used for Rotor

The mesh was made fine with the number of elements of 2859436. To ensure that the resulting mesh is accurate and reliable, both global and local meshing controls are used. Global meshing controls are used to set overall meshing parameters such as the maximum element size and the growth rate of the mesh. These controls are applied to the entire mesh domain.

Local meshing controls, on the other hand, are used to refine the mesh in specific regions of the geometry. This is necessary because the flow field around the Helical Savonius is highly complex and requires a high level of mesh refinement to capture all the details. In this case, faced sizing and body sizing were used as local meshing controls.

Faced sizing involves specifying a target element size for individual faces or surfaces of the geometry. This allows for more control over the mesh in regions where high levels of detail are required. Inflation was also applied along the boundary of turbine.It created the high density of cells near the boundary layer than on the other regions of the other regions of the domain.So, the application of inflation helped to capture the simulation near the boundary layer more accurately.

3.4.3 Turbulence model

In order to analyze turbulent flows in the rotor of the Helical Savonius rotor, a standard k-w turbulence model was used with a logarithmetic surface function. There are two

equations in the k-omega model, which means that it provides two additional equations for solving for turbulent viscosity and specific rate of dissipation of turbulent kinetic energy. By analyzing the flow field around the turbine, we are able to predict turbulence effects more accurately. There are several advantages to using the K-omega model over other turbulence models, such as its ability to accurately capture boundary layer separation, streamline curvature effects, and vortical structures in the wake of the turbine.

3.4.4 Setup

As part of the Fluent, dynamic meshing was performed using 6 degrees of freedom. A dynamic mesh model can be used to simulate flows where the form of a domain changes over time as a result of action on the domain boundary. The use of six degrees of freedom along with dynamic meshes enables aerodynamic forces from the surrounding flow field to control an object's trajectory. Additionally, the dynamic mesh schemes provide the foundation for ANSYS Fluent's dynamic mesh capabilities.
For the boundary conditions , inlet was made velocity inlet and outlet was made pressure outlet. The solver used was pressure based and time was transient as it gives the instantaneous values in each time for each quantity.
The Least Square Discretization (LSD) method was used which is a numerical scheme used for the solution of partial differential equations (PDEs), such as the Navier-Stokes equations in fluid dynamics. The LSD method is a type of finite element method that uses least-squares approximation to discretize the governing equations.
The partial differential equations are discretized using a least-squares approach when using the LSD method with second-order upwind discretization. By combining linear basis functions at each node, a linear approximation of the unknown solution is achieved. By minimizing the least-squares error between the exact solution and the discrete approximation, the coefficients of the basis functions are determined.The resulting system of linear equations is then solved using numerical methods such as the conjugate gradient method or the Gauss-Seidel method. The solution obtained from this process gives an approximation of the dependent variables (such as velocity or pressure) at each node in the mesh, which can be used to analyze and predict the behavior of the fluid flow.

In summary the boundary conditions are as follows:

Inlet	Velocity Inlet
Outlet	Pressure Outlet
Walls	No-slip
Turbine walls	Stationary Blades

Table 3.2: Boundary conditions

3.5 Fabrication

The fabrication of wind turbine can be broke down in the following component.

3.5.1 Blade Profile

The complete blade profile was designed in the SolidWorks surface modelling and the drawing of the blade profile obtained after flattening the respective blade profile was printed in the A0 paper(849 X1189mm) which was later pasted in sheet metal to cut the profile.

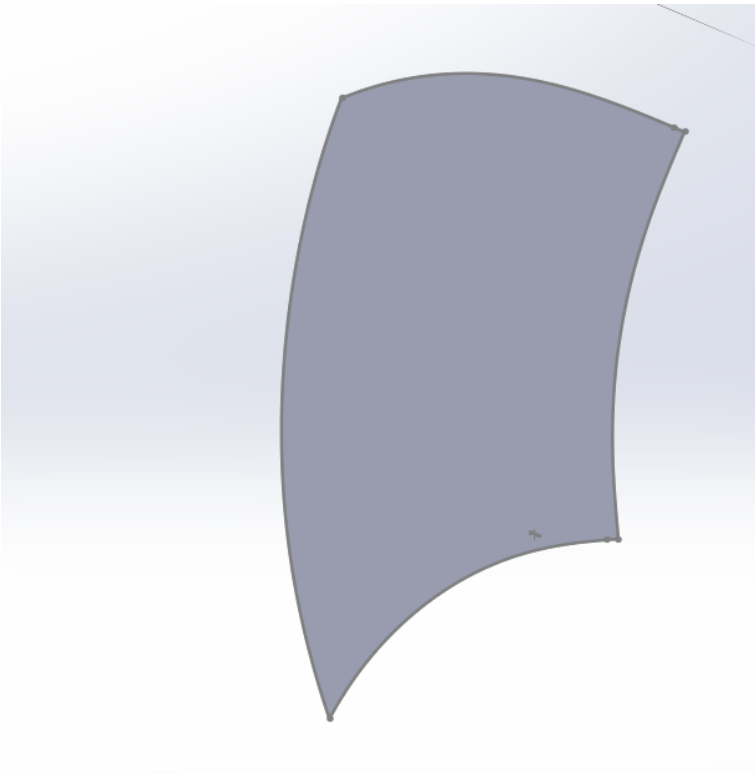

Figure 3.15: Flattened view of blade profile

3.5.2 Helical Profile Guide

In order to guide the sheet metal into the helix ,helical profile guide was necessary.The guide profile was 3d printed.The each slot was of 87.5 mm in height with 8 number in each side. The each side of slots give the helix path to the sheet metal used for the rotor.The slots are riveted into the CPVC pipe and then the sheet metal is placed into the gaps of the slots along with the supporting ribs which was already fabricated.

Figure 3.16: Helical Profile Guide

3.5.3 Shaft

The mild steel shaft of 1.5m and 25.4mm diameter was used according to the design. It was fabricated by machining process in the workshop of Mechanical department by turning and facing on the lathe machine.The clearance of 10 mm on each side is taken for the ease of operation of shaft during the operation of turbine.Bearing mountings are also placed in the shaft for the placement of bearings.

Figure 3.17: Shaft

3.5.4 Supporting Ribs

The blade profile consist of the arc of 124 degree.Using the sheet metal only it will be difficult to hold the sheet metal blades.So supporting ribs were made using the metal stripe of 20mm mild steel flat stripe.The rectangular metal stripes were rolled in the rolling machine to achieve the circle of required radius,which was later cut down into an arc of 124 degree.Similarly those ribs were joined by welding with the bush for making the assembly process easier.

Figure 3.18: Supporting Ribs

3.5.5 Frame

Frame has the length of 4.5ft,width of 4.5 ft and height of 6ft.It supports the helical batch Savonius turbine.It is the mild steel structure with holes and slots which facilitates in assembly of wind rotor.The frame is assembled by the fasteners so the structure was stable to withstand the centrifugal load of the turbine assembly.

Figure 3.19: Frame

3.5.6 Assembly

After the fabrication of entire components, the parts were assembled. At first, the frame was assembled and the mid-section beams were held for the placement of turbine.The bearing housings were also placed.The helical profile guide and CPVC pipe are rivetted and then the supporting ribs were connected to them.The assembly was placed into the shaft and finally the sheet metal was placed into the helical profile for the completion of turbine.

3.6 Testing

Digital anemometers were used to measure the average wind speed. The rotation speed of the turbine was measured using a digital tachometer at different wind speeds as part of the measurement. The dynamic torque of the turbine has been measured using a rope brake dynamometer. In order to accomplish this task, a digital spring balance, dead weights, pulleys, and rope have been used. The details of the instruments are as below.

3.6.1 Measuring Instrument

3.6.1.1 Anemometer

An anemometer is an instrument to measure the wind speed.We used the digital anemometer to measure the wind speed.The detail specification of anemometer is as below:

Make:Smart Sensor

Model No:AR826

Type:Digital

Range:0 m/s-45 m/s

Accuracy:$\pm$0.03

Figure 3.20: Anemometer

3.6.1.2 Tachometer

Tachometer is an instrument to measure the rotational speed.We used the digital tachometer to measure the speed of the shaft.It displays the rotational speed of the overall turbine.It counts the number of times light reflected from the sticker that was stuck on the shaft.The detail specification of tachometer is as below:

Make:ezonedeal

Model No: DT-2234C^{+}

Type: Digital

Range: 2.5 RPM to 99,999 RPM

Accuracy: ± 0.05

Figure 3.21: Tachometer

3.6.1.3 Digital Weight Balance

The detail specification of digital weight balance is as below:

Make:Fuzion Smile

Model No:GM28858

Type:Digital

Range:uptp 50Kg

Accuracy:± 5 10g

Figure 3.22: Digital Weight Balance

3.6.2 Experimental Setup

A 0.6 meter diameter axial fan was used in the testing. The turbine's performance was evaluated by field testing using axial fans at IIEC, Pulchowk Campus since a wind tunnel was not available for the size of the turbine. Wind velocity was accordingly adjusted. A digital anemometer was used to measure wind velocity and a digital tachometer was used to measure rotational speed. In order to test the turbine, axial fans were arranged on a table. The speed of the air was adjusted accordingly and the velocity was noted down using digital anemometer. Using a digital tachometer, the rotational speed of the shaft was measured. The laser of the tachometer was interfered with by the light. As a result, a

reflector was placed in the shaft of the turbine, which solved the interference issue as well as making it easier to take readings from a safe distance without incurring any errors.

3.6.3 Torque measurement

The rope brake dynamometer was designed and fabricated in order to measure torque experimentally. Digital weight balance, Nylon pulley, pulley, and a dead weight were used in the design. The nylon pulley had diameter of 40mm. For torque testing, the rope passing along the groove of the pulley was connected to a digital spring balance and another to a dead weight. As the dead weight was increased, the rotational speed of the turbine kept on decreasing and finally stopped at certain time. After that, the digital weight balance and dead weight reading's were noted down. Finally, the torque was calculated mathematically by using the weight obtained from the digital weight balance, the dead weight and the radius of the pulley.
The formula to calculate the torque is:

$$Torque = (W_1 - W_2) \times 9.81 \times R \tag{3.10}$$

In this equation, W_1 represents the weight measured by the spring balance, W_2 represents the dead weight , R represents the radius of the nylon pulley plus the radius of the rope.

Figure 3.23: Torque measurement

4 CHAPTER FOUR:RESULTS AND DISCUSSION

4.1 CFD Analysis results

The data obtained from the ANSYS Workbench 2021 are listed as follows:

1. Effects of varying tip speed ratio in torque coefficient of the helical rotor
2. Effects of varying tip speed ratio in power coefficient of the helical rotor
3. Effect in rotor angle variation in the torque generation of helical rotor.
4. Velocity and static pressure distribution on helical rotor blade at aspect ratio 0.7.

Above listed data obtained via ANSYS Workbench 2021 are explained as follows:

4.1.1 Effects of varying tip speed ratio in torque coefficient of the helical rotor

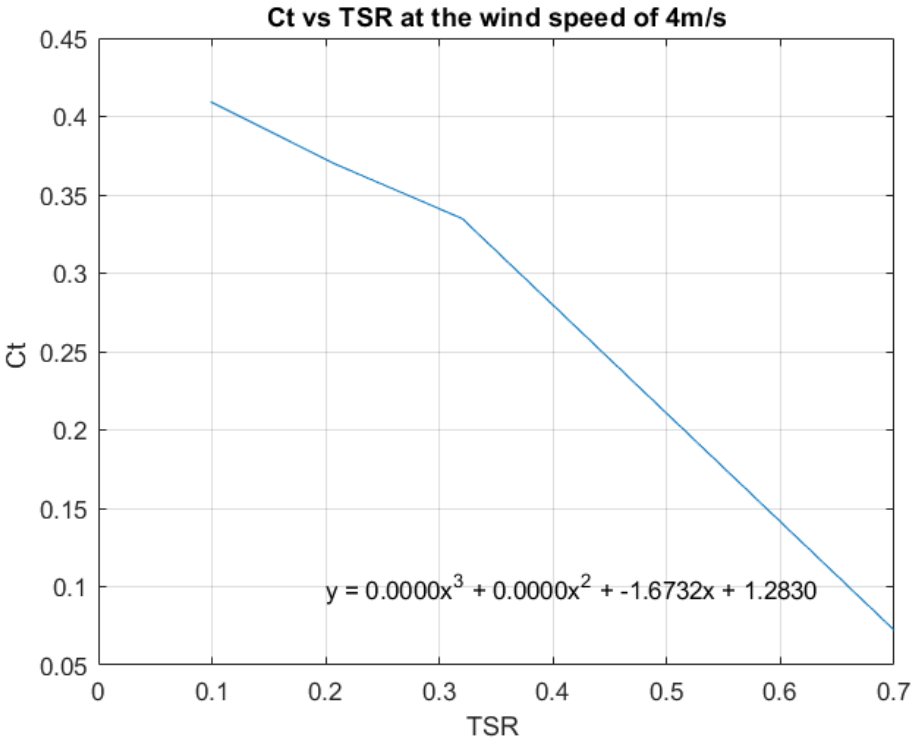

Figure 4.1: Torque coefficient variation with the Tip speed Ratios at 4m/s

According to the figure, the torque coefficient decreases as the tip speed ratio increases. The reason for this is that as the tip speed ratio increases, the RPM increases, which leads to an increase in drag forces within the turbine. Furthermore, higher TSR values result in more turbulent blades, which further reduces torque generation..

4.1.2 Effects of varying tip speed ratio in power coefficient of the helical rotor .

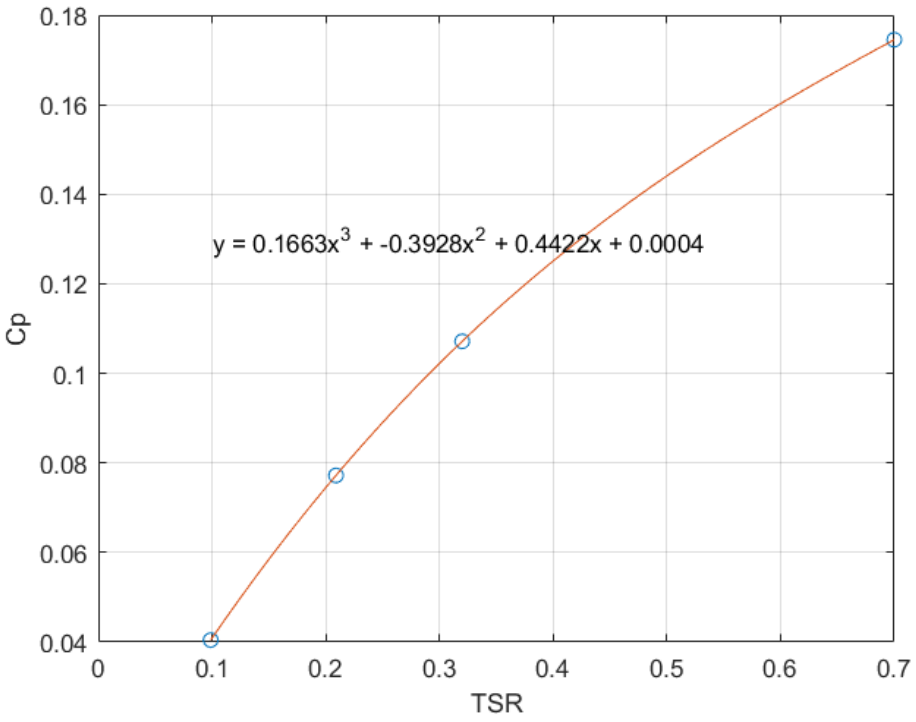

Figure 4.2: Power coefficient variation with the Tip Speed Ratios at 4m/s

When TSR is lower, the helical Savonius turbine produces relatively low torque and power while experiencing low levels of flow separation. In addition to increasing drag and torque, the flow over the blade becomes more turbulent as the TSR increases. By increasing torque, the turbine is able to produce more power, leading to an increase in Cp. So, upto the TSR=0.7 the value of Cp increases with the increase in TSR.

4.1.3 Effect in rotor angle variation in the torque generation of helical rotor.

The variation of torque,torque coefficient at various rotor angles can be studied using the plots and the data presented in the tables below.

Figure 4.3: Torque coefficient variation at different rotor angles at TSR=0.7

Rotor Angle (Degree)	Torque (Nm)	Torque Coefficient (Ct)
0	0.444	0.117
18	1.45	0.383
36	2.16	0.570
54	2.44	0.646
72	2.26	0.599
90	1.52	0.401
108	0.45	0.119
126	0.44	0.117
144	0.79	0.211
162	0.478	0.125
180	0.47	0.124
198	1.45	0.117
216	2.16	0.383
234	2.44	0.570
252	2.26	0.646
270	1.52	0.599
288	0.45	0.401
306	0.44	0.119
324	0.79	0.117
342	0.48	0.211
360	0.47	0.125

Table 4.1: CFD results of Variation of Torque and Torque coefficient with Rotor Angles at TSR=0.7

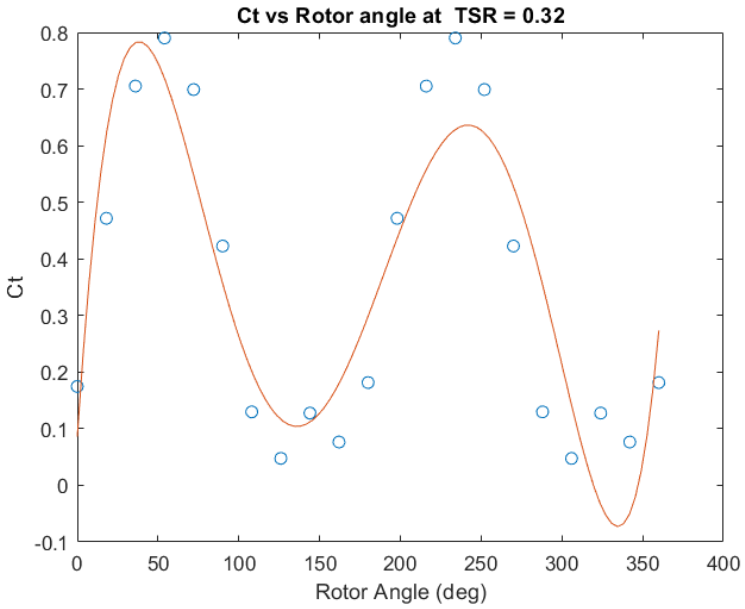

Figure 4.4: Torque coefficient variation at different rotor angles at TSR=0.32

Rotor Angle (Degree)	Torque (Nm)	Torque Coefficient (Ct)
0	0.660	0.174
18	1.785	0.471
36	2.669	0.705
54	2.990	0.790
72	2.646	0.699
90	1.599	0.422
108	0.491	0.129
126	0.180	0.047
144	0.483	0.127
162	0.289	0.076
180	0.687	0.181
198	1.785	0.471
216	2.669	0.705
234	2.990	0.790
252	2.646	0.699
270	1.599	0.422
288	0.491	0.129
306	0.180	0.047
324	0.483	0.127
342	0.289	0.076
360	0.687	0.181

Table 4.2: CFD results of Variation of Torque and Torque Coefficient with Rotor Angle at TSR=0.32

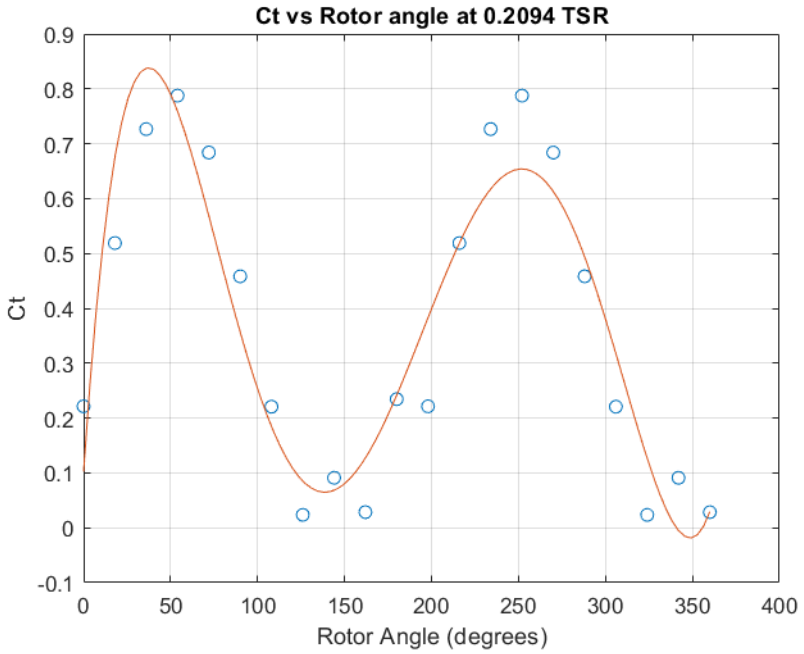

Figure 4.5: Torque Coefficient Variation at Different Rotor Angles at TSR=0.2094

Rotor Angle (Degree)	Torque (Nm)	Torque Coefficient (Ct)
0	0.825	0.221
18	1.935	0.518
36	2.710	0.726
54	2.937	0.787
72	2.550	0.683
90	1.709	0.458
108	0.823	0.220
126	0.087	0.0235
144	0.339	0.091
162	0.106	0.028
180	0.874	0.234
198	0.825	0.221
216	1.935	0.518
234	2.710	0.726
252	2.937	0.787
270	2.550	0.683
288	1.709	0.458
306	0.823	0.220
324	0.087	0.023
342	0.339	0.091
360	0.106	0.028

Table 4.3: CFD results of Variation of Torque and Torque Coefficient with Rotor Angle at TSR=0.2094

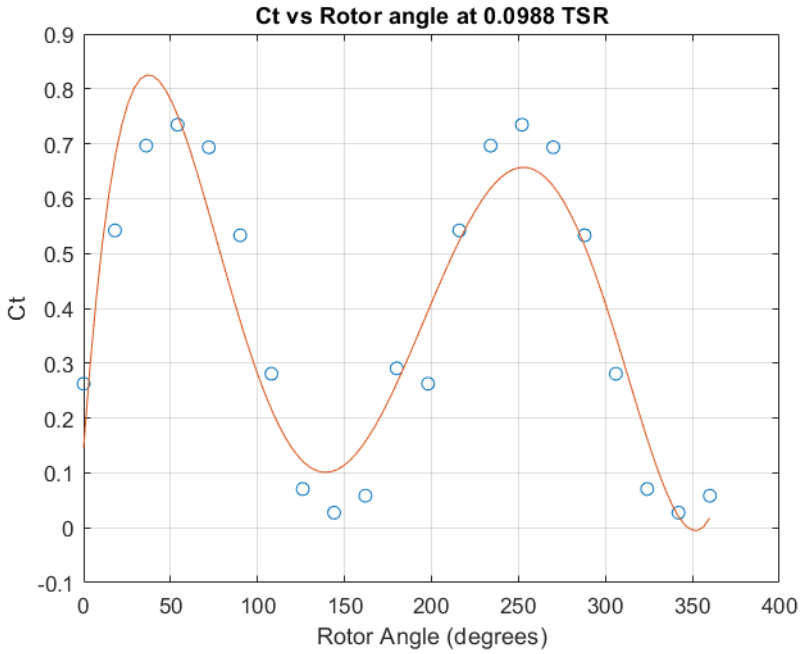

Figure 4.6: Variation of Torque Coefficient at Different Rotor Angles at TSR=0.0988

Rotor Angle (Degree)	Torque (Nm)	Torque Coefficient (Ct)
0	0.979	0.262
18	2.021	0.541
36	2.597	0.696
54	2.740	0.734
72	2.586	0.693
90	1.988	0.533
108	1.047	0.280
126	0.263	0.070
144	0.102	0.0272
162	0.218	0.0584
180	1.083	0.290
198	0.979	0.262
216	2.021	0.541
234	2.597	0.696
252	2.740	0.734
270	2.586	0.693
288	1.988	0.533
306	1.047	0.280
324	0.263	0.070
342	0.102	0.027
360	0.218	0.058

Table 4.4: CFD Results of Variation of Torque and Torque coefficient with Rotor Angle at TSR=0.0988

Tip Speed Ratio	Power(W)	Torque(N-m)	C_p	C_t
0.7	5.054	2.448	0.1745	0.24
0.32	3.103	2.990	0.107	0.334
0.209	2.236	2.9377	0.0772	0.369
0.0988	1.171	2.74	0.0404	0.4093

Table 4.5: Variation of Power Coefficient and Torque Coefficient at Various TSRs when Wind Speed =4 m/s and Rotor angle=54°.

According to the above plots and tables, the maximum torque and power can be obtained with a rotor at an angle of 54 degrees.

4.1.4 Pressure and velocity distribution on the Savonius rotor blade

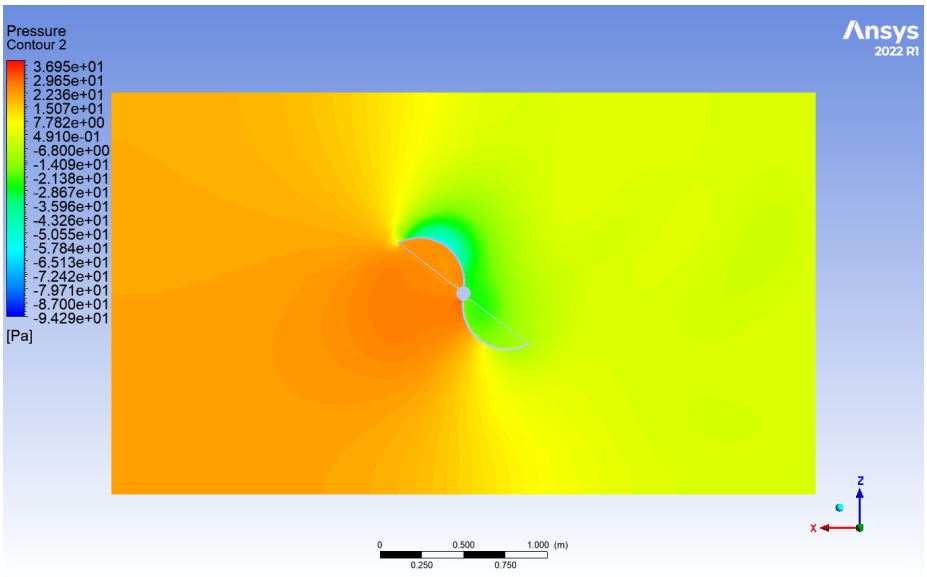

Figure 4.7: Pressure contour at the Wind Speed of 4 m/s at the TSR=0.7

The maximum and minimum pressure are -9.42 Pa and 36.95 Pa respectively at the average wind speed of 4 m/s at the Tip speed ratio of 0.7. Because of the helical shape of the Savonius rotor there is pressure difference in advancing blade and returning blade of the rotor where due to difference in pressure causes generation of torque.

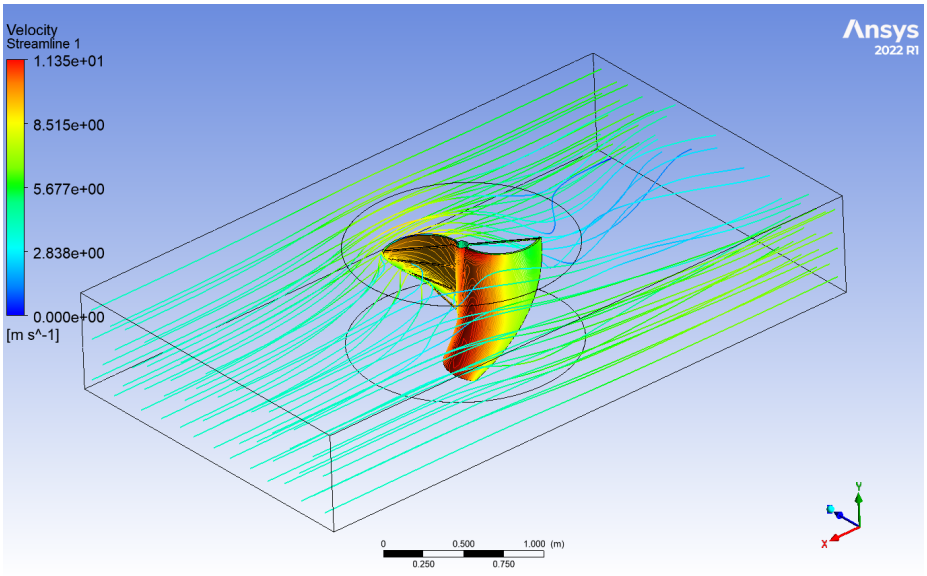

Figure 4.8: Velocity Contour at the Wind Speed of 4 m/s at the TSR=0.7

The figure above demonstrates the velocity distribution of the air at the average wind speed of 4 m/s with the tip speed ratio of blade of 0.7. According to the contour, maximum velocity of air is available at the tip of the blades and minimum at the shaft of the rotor.

4.2 Results from the experiment

The turbine was tested at IIEC, Pulchowk with the axial fans provided by Center of Energy Studies.The testing was done at various wind speeds and data was recorded.

4.2.1 Comparison of average wind speed and rpm of turbine

During the testing , the results of average wind speed,their respective rotational speeds and torques were noted at a certain time interval.The wind speed was ranging from 1.1 m/s to 4.0 m/s . So, total eight data sets were noted down ranging from 1.1 m/s to 4.0 m/s.The direction of rotation of turbine was in anticlockwise direction because the right blade was concave and the left one was convex.

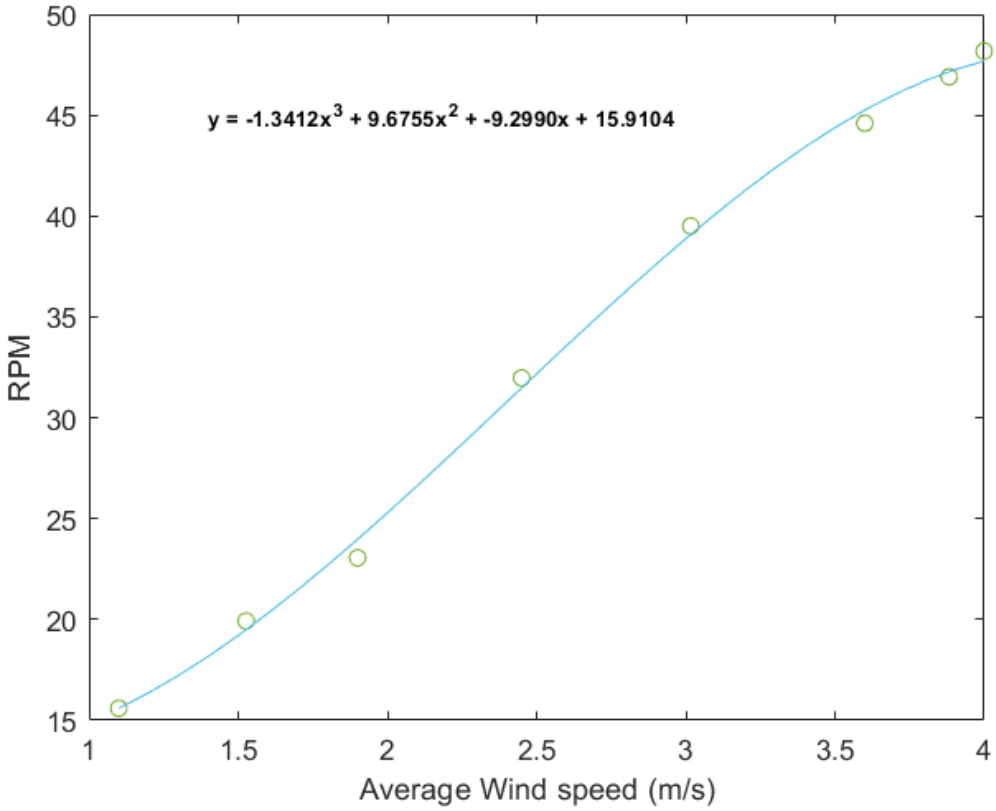

Figure 4.9: Average Wind Speed vs RPM

Average Wind Speed(m/s)	**RPM**
1.1	15.593
1.5265	19.25
1.9	23.0525
2.45	31.975
3.0166	39.506
3.6	44.6
3.8825	46.9
4	48.18

Table 4.6: Average Wind Speed vs RPM of Turbine

4.2.2 Torque of turbine at different average wind speed

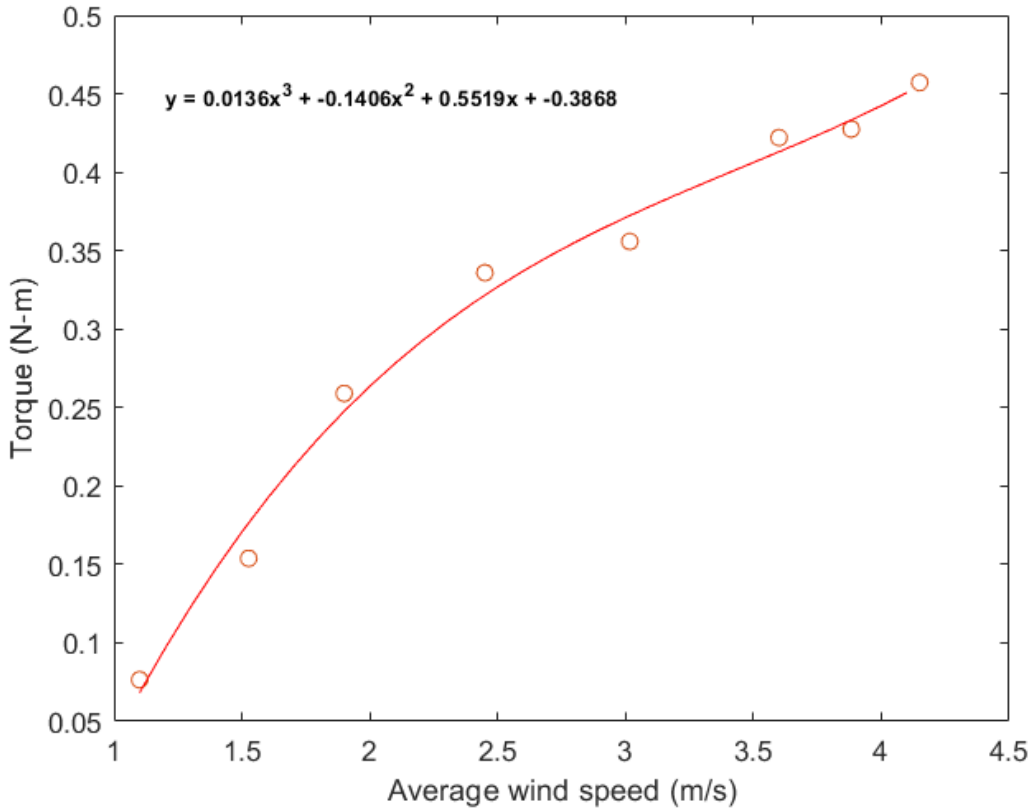

Figure 4.10: Average Wind Speed vs Torque

Average wind speed(m/s)	Torque(N-m)
1.10	0.0765
1.53	0.153
1.90	0.258
2.45	0.335
3.01	0.355
3.61	0.4220
3.88	0.427
4.00	0.457

Table 4.7: Torque of turbine at different average wind speed

The plot shows the details about the torque generated by the blade with respect to average wind speed. It is evident that the torque generated is directly proportional to the wind speed. Also, the torque generated is increased sharply as the rotational speed corresponding to the average wind speed is also increasing.

4.2.3 Torque of turbine at different rpm

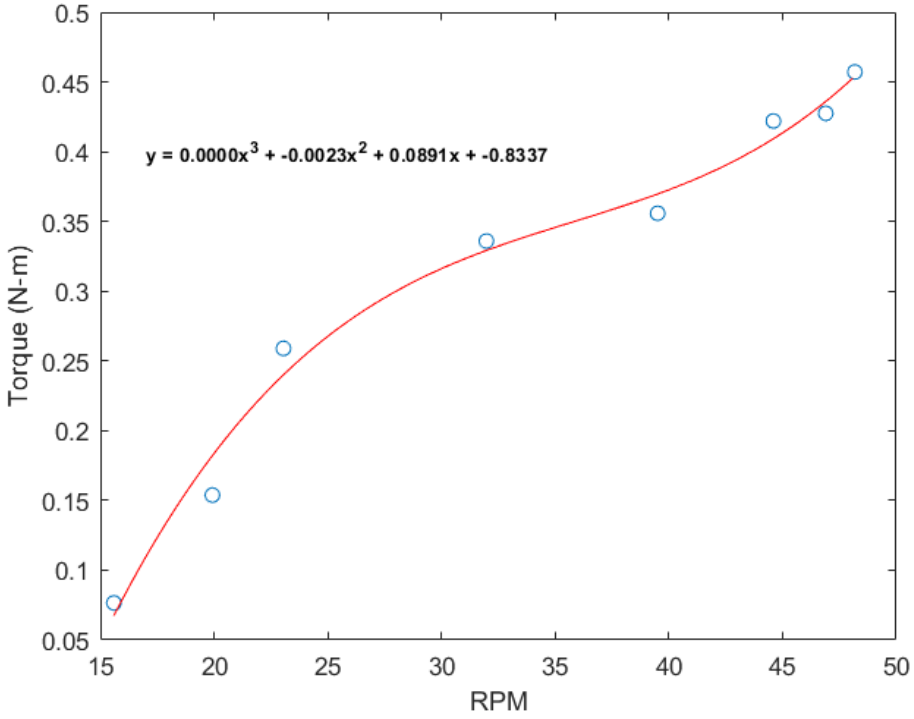

Figure 4.11: RPM vs Torque

RPM	Torque(N-m)
15.59	0.0765
19.93	0.153
23.053	0.258
31.97	0.335
39.50	0.355
44.60	0.4220
46.90	0.427
48.20	0.457

Table 4.8: Torque of turbine at Different Average Wind Speed

As in the plot above, the torque generated by the rotor increases with the increase in the rotor speed. It is clear that torque generated by the rotor is the function of rotational speed. The relation between torque and rpm is observed non-linear.

4.2.4 Power of turbine at different average wind speed

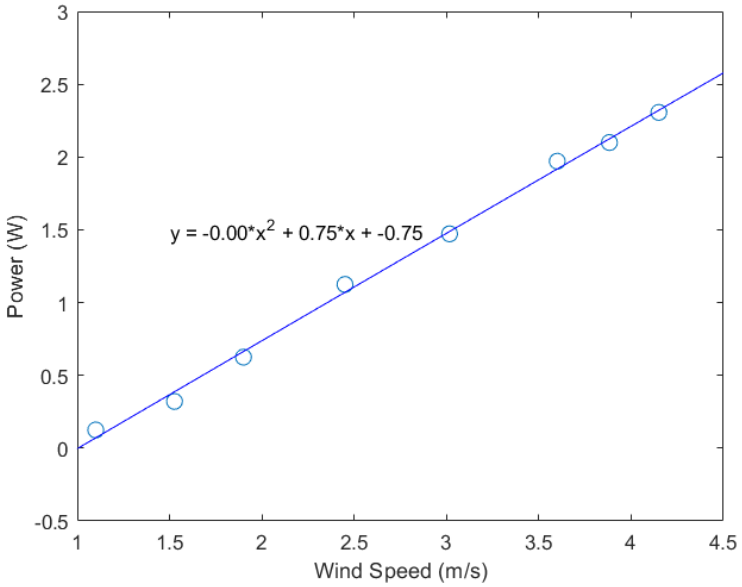

Figure 4.12: Power vs Average Wind Speed(m/s)

It is noticed that the power produced linearly increases with the wind speed.Due to the mechanical losses and Betz's limit , there is difference in experimentally produced power and the theoretical power produced by the wind turbine.

Average Wind Speed(m/s)	**Power(W)**
1.1	0.124
1.5265	0.320
1.9	0.624
2.45	1.124
3.0166	1.471
3.6	1.970
3.883	2.098
4.0	2.306

Table 4.9: Power of turbine at different average wind speed

4.2.5 Performance of turbine at different TSR

Various tip speed ratios were also tested at 4.0 m/s for the turbine at the same wind speed but with varying rotational speed in order to determine its performance. A rope brake dynamo meter was used to adjust the turbine's rotation speed.
The test results are as follows:

Average wind Speed(m/s)	Tip speed ratio	Torque(N-m)	Cp	Ct
4.0	0.630	0.551	0.093	0.0147
4.0	0.321	0.295	0.0254	0.0791
4.0	0.209	0.406	0.0228	0.108
4.0	0.098	0.495	0.013	0.132

Table 4.10: Characteristics of Turbine at Different TSRs

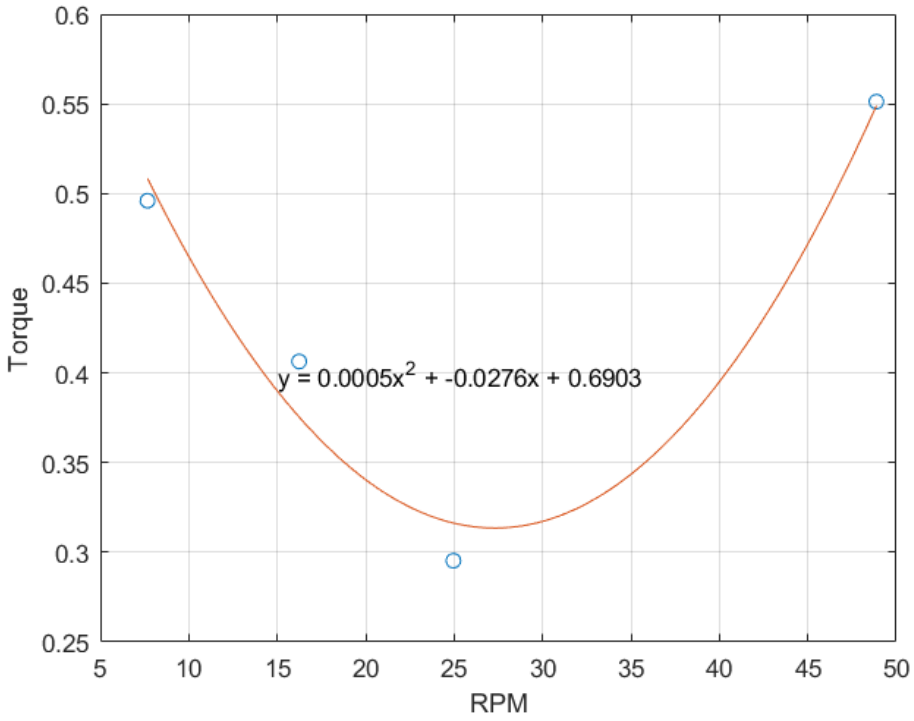

Figure 4.13: Torque vs RPM at various TSRs at Wind Speed of 4 m/s

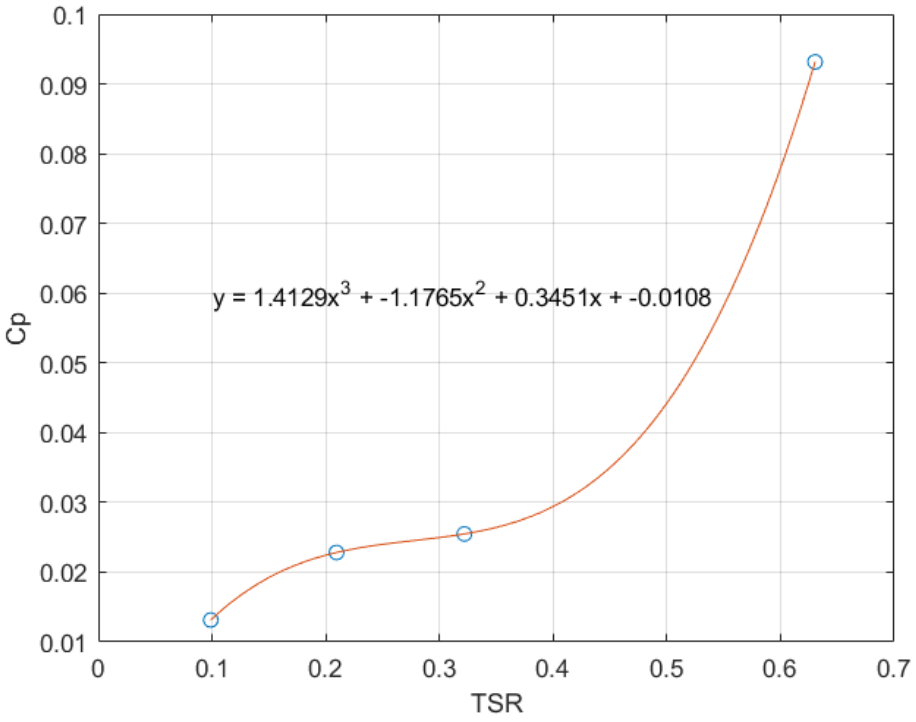

Figure 4.14: Power Coefficient vs TSR at Wind speed of 4 m/s

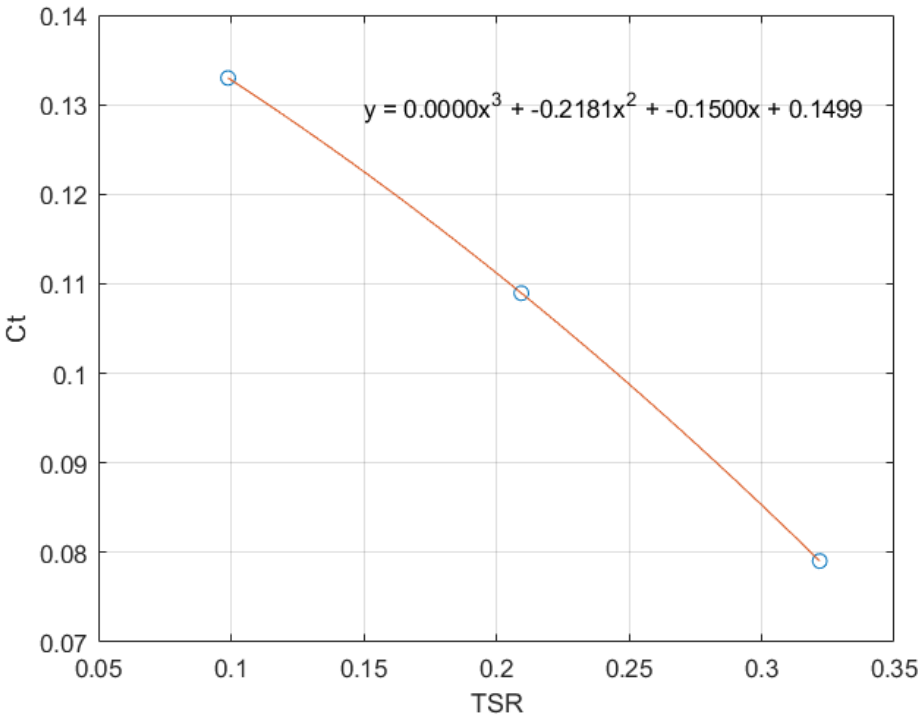

Figure 4.15: Torque coefficient vs TSR at Wind Speed of 4 m/s

4.3 Comparison of Experimental and CFD results

4.3.1 Comparison of Power coefficient vs TSR from CFD and experimental analysis

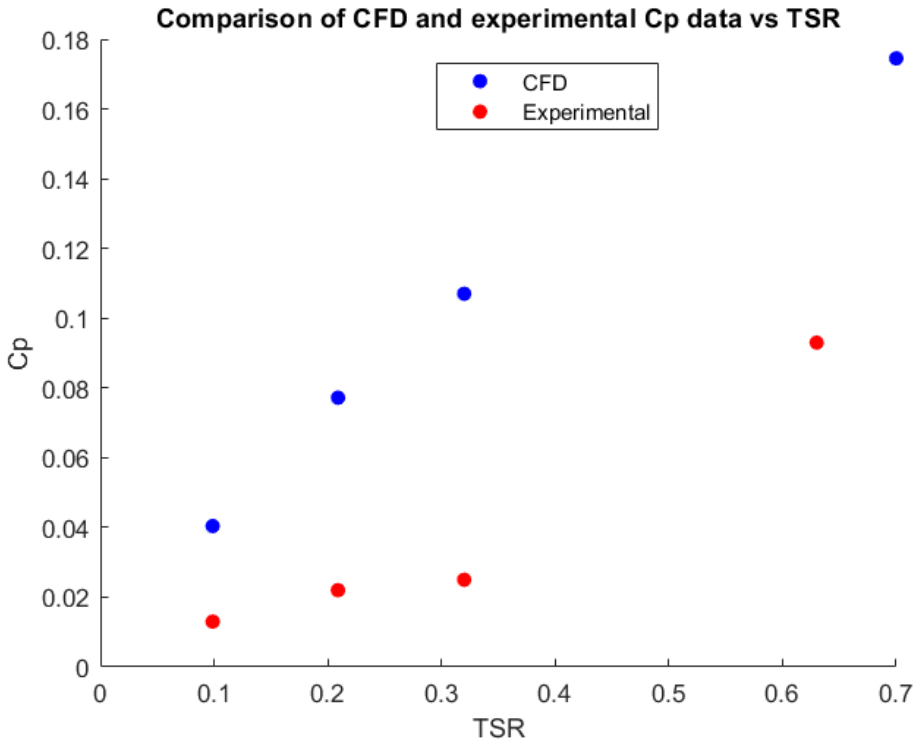

Figure 4.16: Comparison of Power coefficient vs TSR from CFD and Experimental analysis

The analysis of the experimental results and computational fluid dynamics (CFD) simulations indicate that the power coefficient (Cp) increases with an increase in the tip speed ratio (TSR) for the tested wind turbine. This trend is consistent with different literature and confirms the expected performance of the wind turbine. However, it should be noted that the test was limited by the bearing friction at the wind speed of 4 m/s, preventing the observation of the complete nature of the curve.

4.3.2 Comparison of Torque coefficient vs TSR from CFD and Experimental analysis

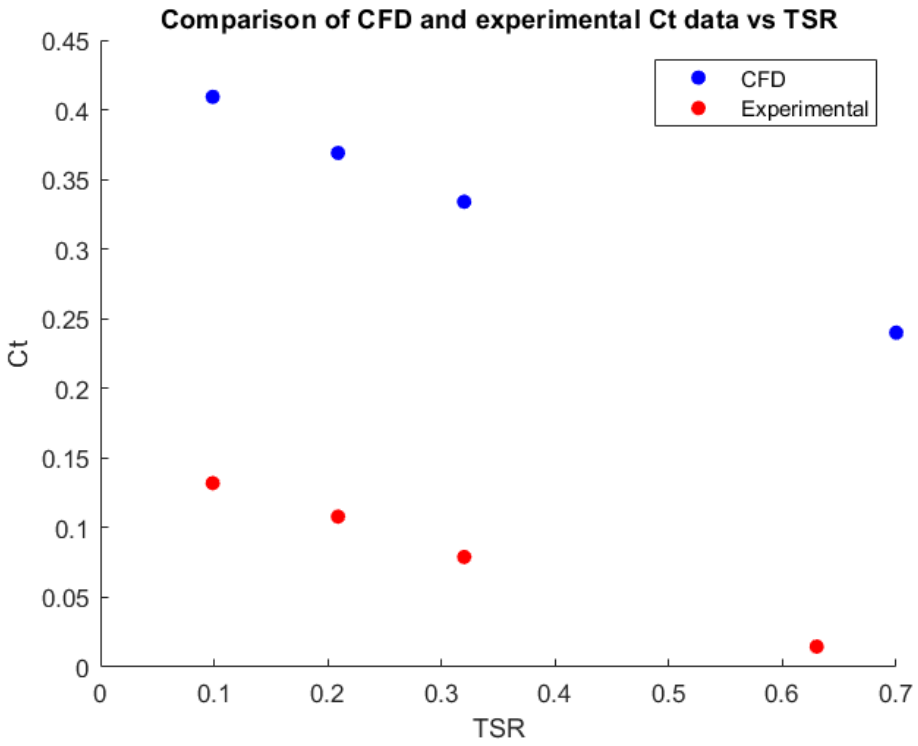

Figure 4.17: Comparison of Torque coefficient vs TSR from CFD and Experimental analysis

Based on the analysis of the experimental data and CFD simulation, it was observed that the value of torque coefficient (Ct) decreases with an increase in the tip speed ratio (TSR) for the tested Helical Savonius Bach type wind turbine. At lower TSR values, the incoming wind flow strikes the blades at a higher angle of attack, resulting in a greater amount of wind energy being transferred to the rotor and converted into mechanical energy. As the TSR increases, the angle of attack decreases, causing a reduction in the amount of wind energy transferred to the rotor. This reduction in the amount of energy results in a decrease in the value of Ct.

4.4 Cost Analysis

The overall cost of the project was Rs 48,050.The cost for the overall project is shown in the table below:

Particulars	**Material**	**Size**	**Quantity**	**Cost**(Rs)
UP fila PLA	PLA	-	1kg	6500 /-
CPVC Pipe	CPVC	50.8 mm	3m	4500 /-
Sheet metal(0.20mm)	GI	0.20 mm	20ft	6000 /-
Shaft	MS	25.4 mm ϕ	1	8000 /-
Cylindrical Rod(47mm ϕ)	MS	47 mm ϕ	230mm	500 /-
Slotted Angle Beam	MS	20 ft	4	6400 /-
Roller Bearing	6002	4mm ϕ ID	2	700 /-
Square pillow block bearing	6500c	20mm ϕ ID	1	2200 /-
Thrust Bearing	-	20mm ϕ ID	1	1200 /-
20mm rectangular stripe	MS	20 ft	3	2400 /-
M6 Allen screw	-	12mm	20	300 /-
M10 nut Bolt	-	20mm	100	600 /-
Rivet	Aluminimum	4mm	200	800 /-
Welding Rod	Iron	-	20	200 /-
Nylon Shaft	Nylon	38mm	305mm	350 /-
Digital Balance	-	-	1	400 /-
Tachometer	-	-	1	2000 /-
Miscellaneous	-	-	-	5000 /-
Total				48,050/-

Table 4.11: Cost Breakdown

5 CHAPTER FIVE: CONCLUSIONS,LIMITATIONS AND RECOMMENDATIONS

5.1 Conclusions

The main conclusions from the project are as follows:

1. Turbine operating at the average wind speed of 4.0 m/s, the coefficient of performance (C_p) was found to be 0.1071 numerically and 0.025884 experimentally at the (TSR) of 0.32. Both numerically and experimentally, the C_p increased with increasing TSR. The torque coefficient (C_t) was found to be higher at the low tip speed and goes on decreasing at higher tip speed ratios both numerically and experimentally. This difference in CFD and experimental values is due to the friction in bearing which avoided the turbine to rotate freely and eventually decrease the power.

2. Although the overall power coefficient of the turbine is low, it has a wide range of applications. The cut-in speed of the turbine is 1m/s, so it can be applicable to locations where the wind speed is very low. Also, the wind direction has no effect on the rotation of the turbine because of its helical shape and twist in 90 degrees.

3. This project demonstrates the practical applications of Savonius turbines in the field of renewable energy and presents opportunities for future research and development. With continued efforts to optimize the design and scale up the system, Savonius turbines have the potential to provide sustainable solutions for water supply and irrigation systems in various parts of Nepal.

5.2 Limitations

1. Operation of reciprocating pump was not completed due to time constraints.

2. The appropriate testing facility was not available.

5.3 Recommendations

Based on the comprehensive study conducted during project , it has been demonstrated that Helical Savonius wind turbine has a wide range of applications. It is still possible to

conduct detailed research to make wind energy more economical and reliable. As noted below, there is ample space for future work.

1. Combination of Helical Savonius and Darrieus wind turbine could increase the performance of wind turbine.
2. Installation of end plates can increase the overall efficiency of the turbine. For that the fabrication of blades must be done carefully.
3. Fabrication defects might have reduced the efficiency significantly so, if better fabrication process are followed, efficiency can be increased accordingly.
4. The use of torque sensor instead of rope brake dynamometer and load cell can give better results.
5. The appropriate testing facility for the wind turbine can be fruitful to get better results and performance evaluation.

References

Bartaula, P., & Shakya, S. R. (2020). Design and numerical modelling of vertical axis helical wind turbine for highway application.

Chang, T.-L., Tsai, S.-F., & Chen, C.-L. (2021). Optimal design of novel blade profile for savonius wind turbines. *Energies*, *14*(12), 3484.

Damak, A., Driss, Z., & Abid, M. (2018). Optimization of the helical savonius rotor through wind tunnel experiments. *Journal of Wind Engineering and Industrial Aerodynamics*, *174*, 80–93.

Ghosh, P., Kamoji, M., Kedare, S., & Prabhu, S. (2009). Model testing of single-and three-stage modified savonius rotors and viability study of modified savonius pump rotor systems. *International journal of green energy*, *6*(1), 22–41.

Goh, S. C., & Schlüter, J. U. (2016). Numerical simulation of a savonius turbine above an infinite-width forward facing step. *Wind Engineering*, *40*(2), 134–147.

Hamzah, I., Prasetyo, A., Tjahjana, D. P., & Hadi, S. (2018). Effect of blades number to performance of savonius water turbine in water pipe. In *Aip conference proceedings* (Vol. 1931, p. 030046).

Kamoji, M., Kedare, S., & Prabhu, S. (2009b). Performance tests on helical savonius rotors. *Renewable Energy*, *34*(3), 521–529.

Kamoji, M., Kedare, S. B., & Prabhu, S. (2009a). Experimental investigations on single stage modified savonius rotor. *Applied Energy*, *86*(7-8), 1064–1073.

Kedare, S., & Date, A. (1990). Performance characteristics of a reciprocating wind machine. *Journal of wind engineering and industrial aerodynamics*, *34*(1), 1–25.

Khammas, F., Hussein Suffer, K., Usubamatov, R., & Mustaffa, M. T. (2015). Overview of vertical axis wind turbine (vawt) is one of the wind energy application. *Applied Mechanics and Materials*, *793*, 388–392.

Kumar, P. M., Sivalingam, K., Narasimalu, S., Lim, T.-C., Ramakrishna, S., & Wei, H. (2019). A review on the evolution of darrieus vertical axis wind turbine: Small wind turbines. *Journal of Power and Energy Engineering*, *7*(4), 27–44.

Laudari, R., Sapkota, B., & Banskota, K. (2018). Wind farming feasibility assessment in 16 locations of nepal. *Invertis Journal of Renewable Energy*, *8*(4), 179–191.

Lukiyanto, Y. (2016). A couple of savonius wind mill and centrifugal reaction pump as a wind energy water pump system. In *Applied mechanics and materials* (Vol. 836, pp. 299–303).

Modi, V., & Fernando, M. (1989). On the performance of the savonius wind turbine.

Nayeem, S., Kumar, B. P., Bhaskar, B. A., Jnanendra, A., & Kumar, K. V. (2019). Design and fabrication of water pumping system using wind mill. *International Journal of Management, IT and Engineering*, *9*(5), 140–152.

Oghoghorie, O., Ebunilo, P. O., & Orhorhoro, E. K. (2020). Development of a savonius vertical axis wind turbine operated water pump. *Journal of applied research on industrial engineering*, *7*(2), 190–202.

Parrondo, J. L., Velarde, S., & Santolaria, C. (1998). Development of a predictive maintenance system for a centrifugal pump. *Journal of Quality in Maintenance Engineering*.

Peimani, H. (2021). *Appropriate technologies for removing barriers to the expansion of renewable energy in asia: Vertical axis wind turbines* (Tech. Rep.). ADBI Working Paper Series.

Permadi, M., Andari, G., Sapsal, M., et al. (2019). Prototype design of wind power water pump for irrigation. In *Iop conference series: Earth and environmental science* (Vol. 343, p. 012200).

Premkumar, T. M., Sivamani, S., Kirthees, E., Hariram, V., & Mohan, T. (2018). Data set on the experimental investigations of a helical savonius style vawt with and without end plates. *Data in brief*, *19*, 1925–1932.

Rajput, R. (1998). *A textbook of hydraulic machines*. S. Chand Publishing.

Rusenko, A., Hontz, D., Zhang, A., Norton, J., & Erdman, M. (2014). Vertical axis wind turbine to power a well pump.

Saad, A. S., El-Sharkawy, I. I., Ookawara, S., & Ahmed, M. (2020). Performance enhancement of twisted-bladed savonius vertical axis wind turbines. *Energy Conversion and Management*, *209*, 112673.

Salim, E., Yahya, W., Danardono, D., & Himawanto, D. (2015). A study of the influence of guide vane design to increase savonius wind turbine performance. *Modern Applied Science*, *9*(11), 222.

Vignesh, J., Christopher, A. S., Albert, T., Selvan, C. P. T., & Sunil, J. (2020). Design and fabrication of vertical axis wind mill with solar system. *Materials Today: Proceedings*, *21*, 10–14.

Wadhai, P. V., & Rangari, D. (n.d.). Design and development of hybrid power generation system.

Wenehenubun, F., Saputra, A., & Sutanto, H. (2015). An experimental study on the performance of savonius wind turbines related with the number of blades. *Energy procedia*, *68*, 297–304.

Wijianti, E., Setiawan, Y., et al. (2020). Experimental study of helical savonius rotor profiles with different number of blade. In *Iop conference series: Earth and environmental science* (Vol. 599, p. 012009).

YİĞİT, C. (2020). Optimization of the s-rotor savonius wind turbine. *Sakarya University Journal of Science*, *24*(6), 1216–1222.

Zemamou, M., Aggour, M., & Toumi, A. (2017). Review of savonius wind turbine design

and performance. *Energy Procedia*, *141*, 383–388.

Zingman, A. A. O. (2007). *Optimization of a savonius rotor vertical-axis wind turbine for use in water pumping systems in rural honduras* (Unpublished doctoral dissertation). Massachusetts Institute of Technology.

APPENDICES

Figure 5.1: Anemometer

Figure 5.2: Tachometer

Figure 5.3: Digital Weight Balance

Figure 5.4: Blade Fabrication

Figure 5.5: Fabrication of shaft on lathe

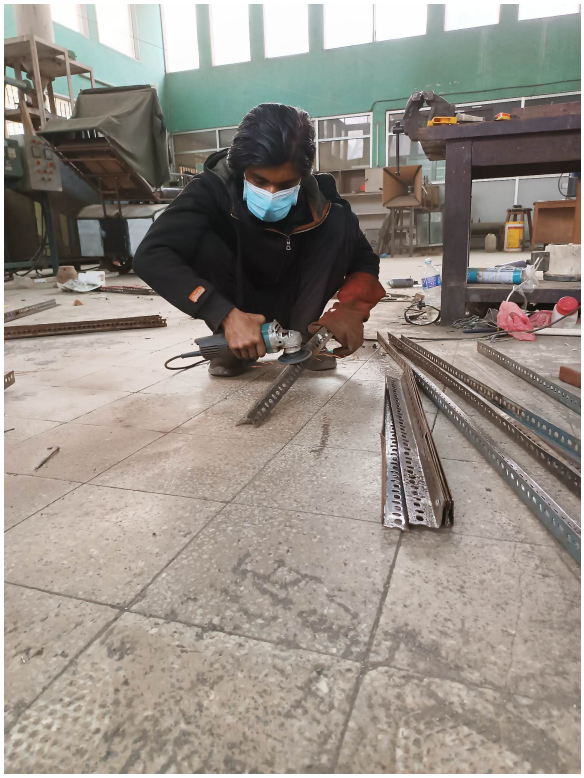

Figure 5.6: Frame Fabrication

Figure 5.7: Fabrication of support for blade

Figure 5.8: Frame Setup

Figure 5.9: Experimental Setup

Figure 5.10: Dynamic Torque Testing

Figure 5.11: Measuring Wind velocity using Anemometer

Figure 5.12: Measuring RPM of Turbine

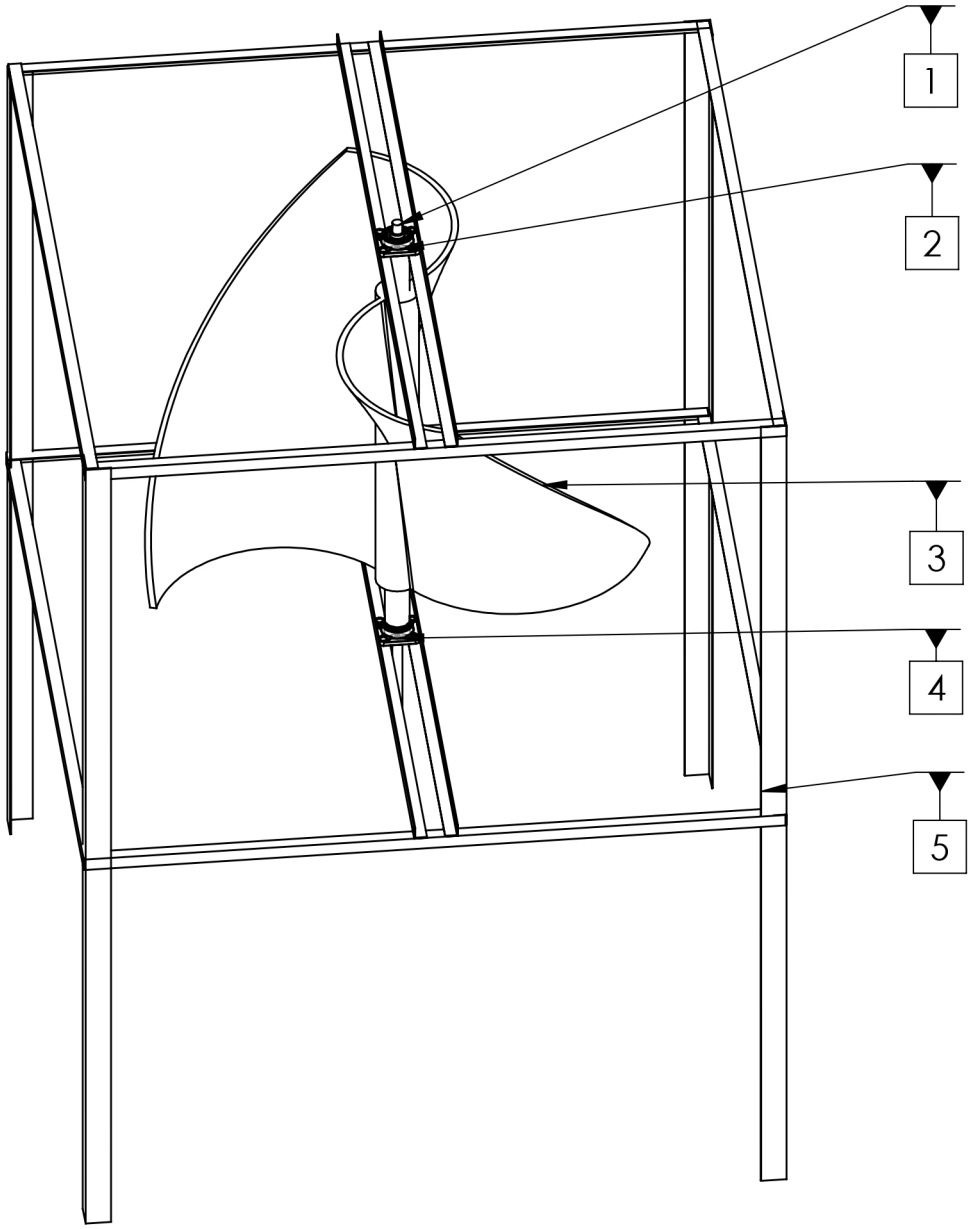

Part No	Part Name	Quantity	Material
5	Frame	1	MS
4	Thrust bearing	1	
3	Blade	2	GI sheet
2	Pillow block bearing	1	
1	Shaft	1	MS

Sheet No=1	Scale 1:15	Assembly Design

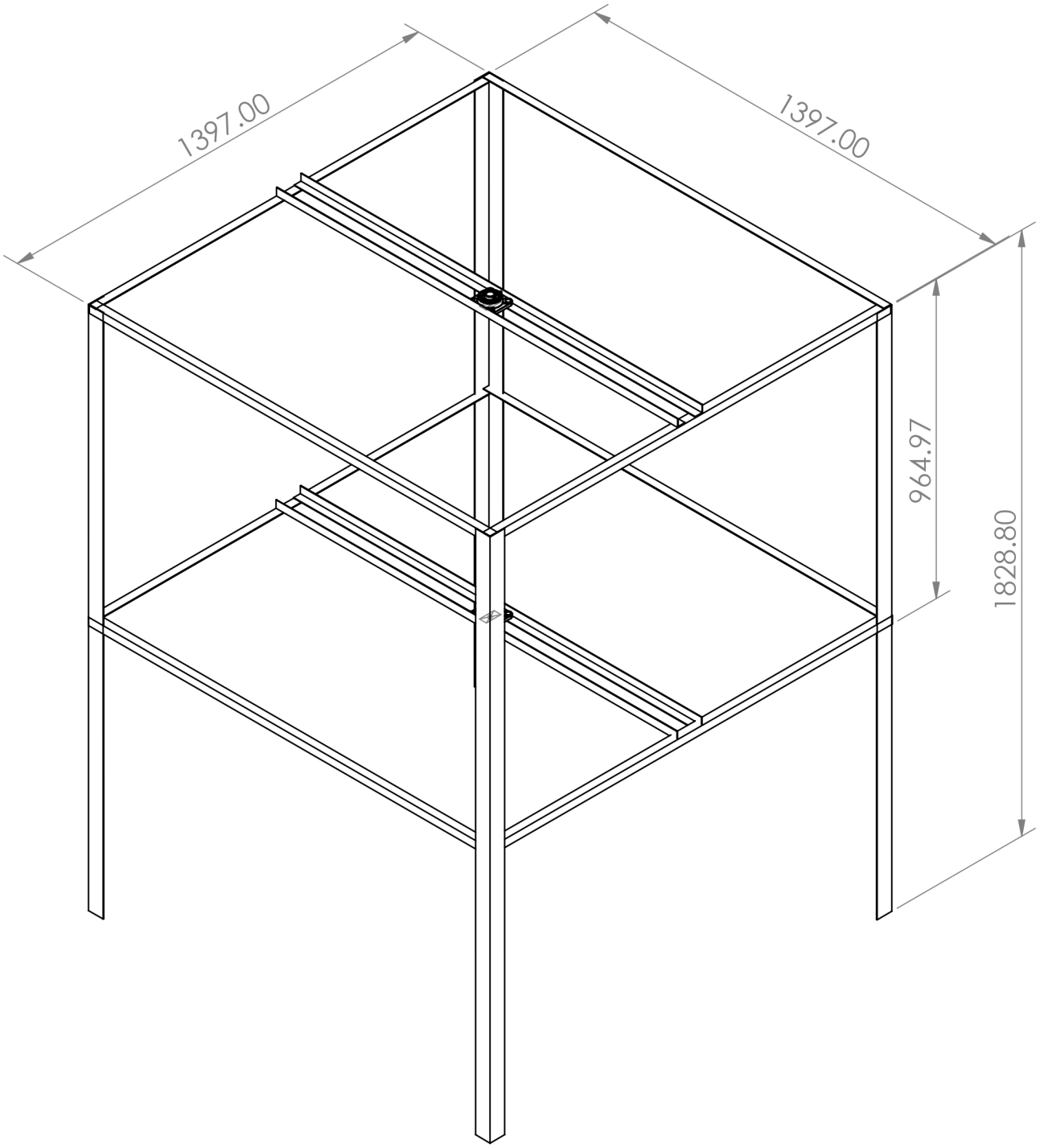

1	Frame Structure	1	MS
Part No	Part Name	Quantity	Material

All dimensions are in mm	Sheet No=2	Scale 1:15	Frame Assembly

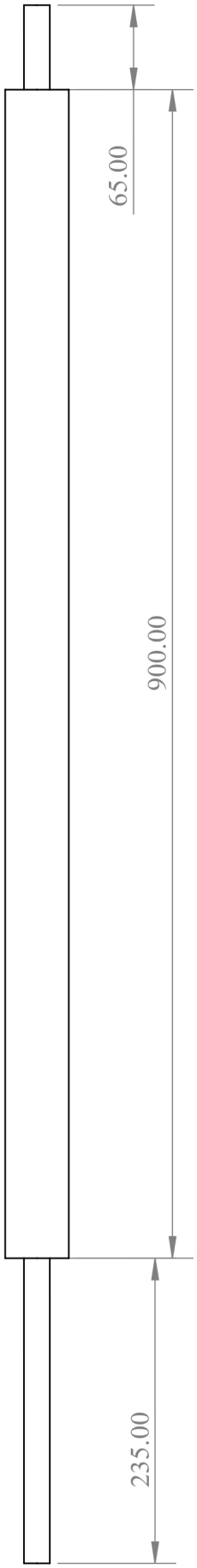

Fig i: Front View

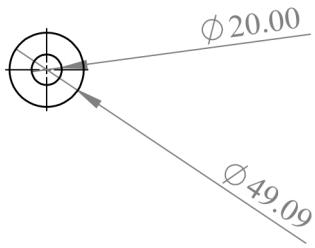

Fig ii: Top View

1	Shaft	1	MS
Part No	Part Name	Quantity	Material

All dimensions are in mm	Sheet No=3	Scale 1:50	Shaft Drawing

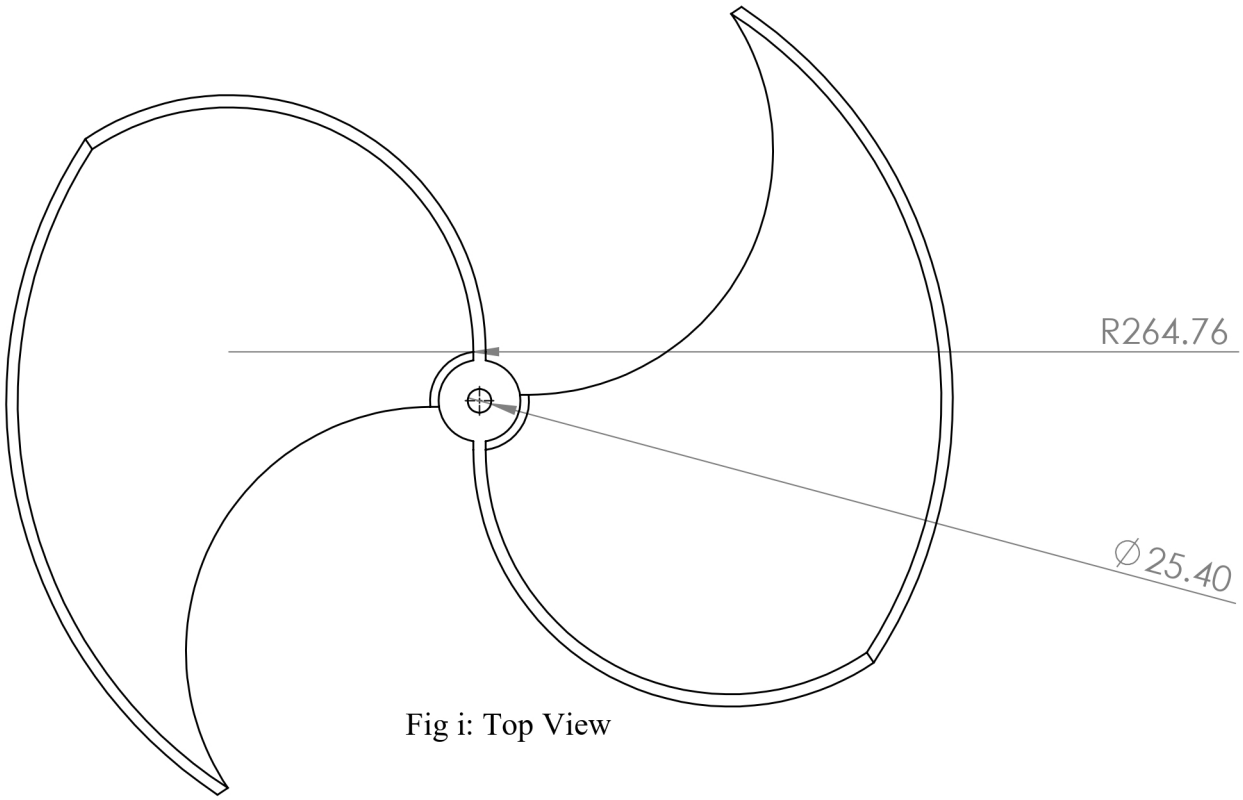

Fig i: Top View

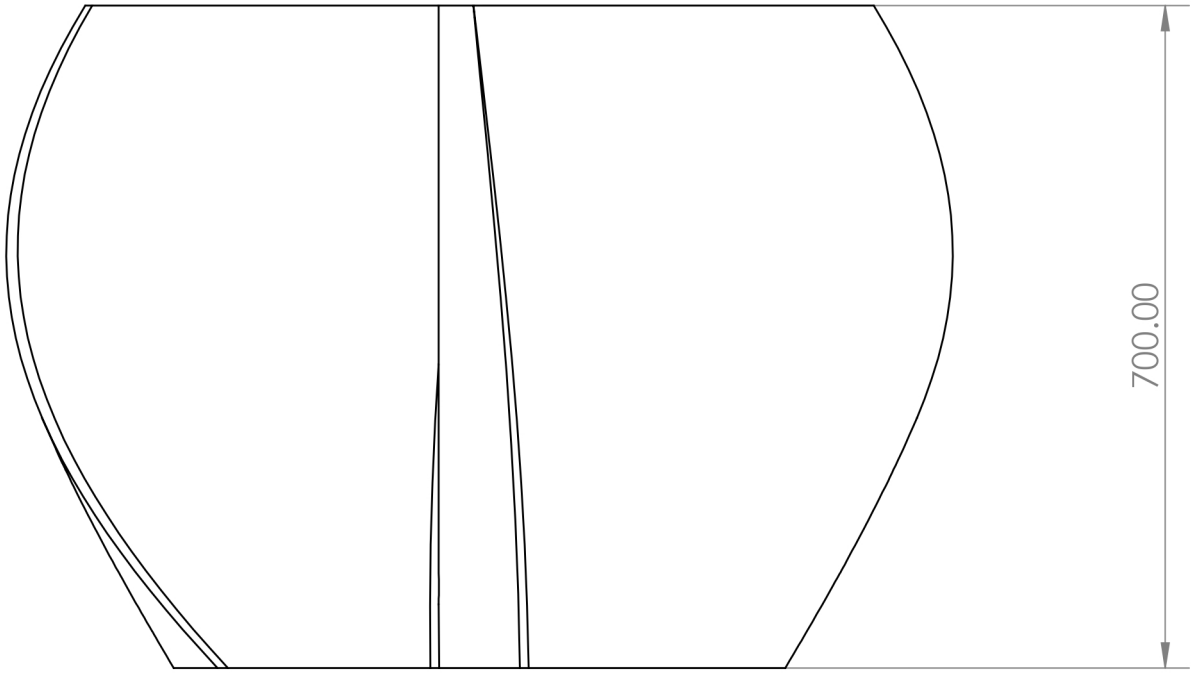

Fig ii: Front View

1	Blades	1	GI
Part No	Part Name	Quantity	Material

All dimensions are in mm	Sheet No=4	Scale 1:8	Blades Drawing

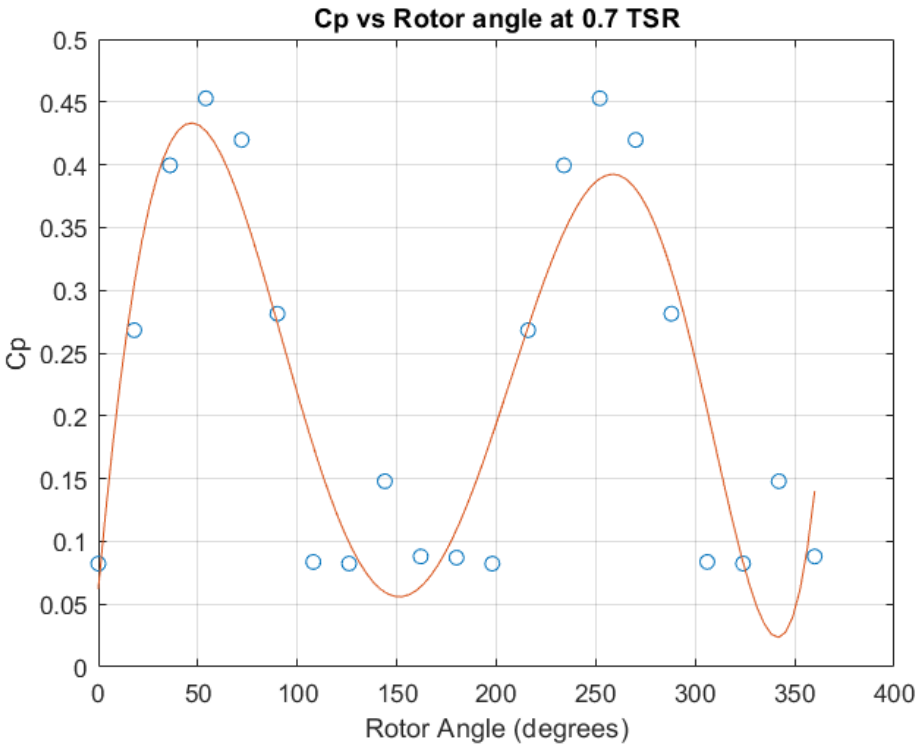

Figure 5.13: Variation of Power coefficient at different rotor angles at TSR=0.7

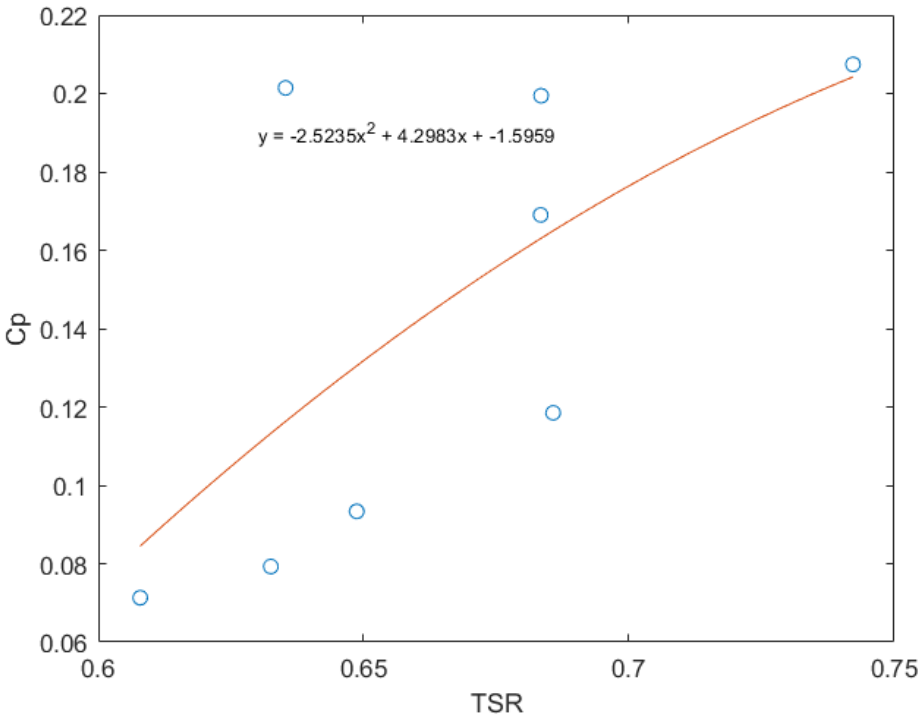

Figure 5.14: Power coefficient vs TSR

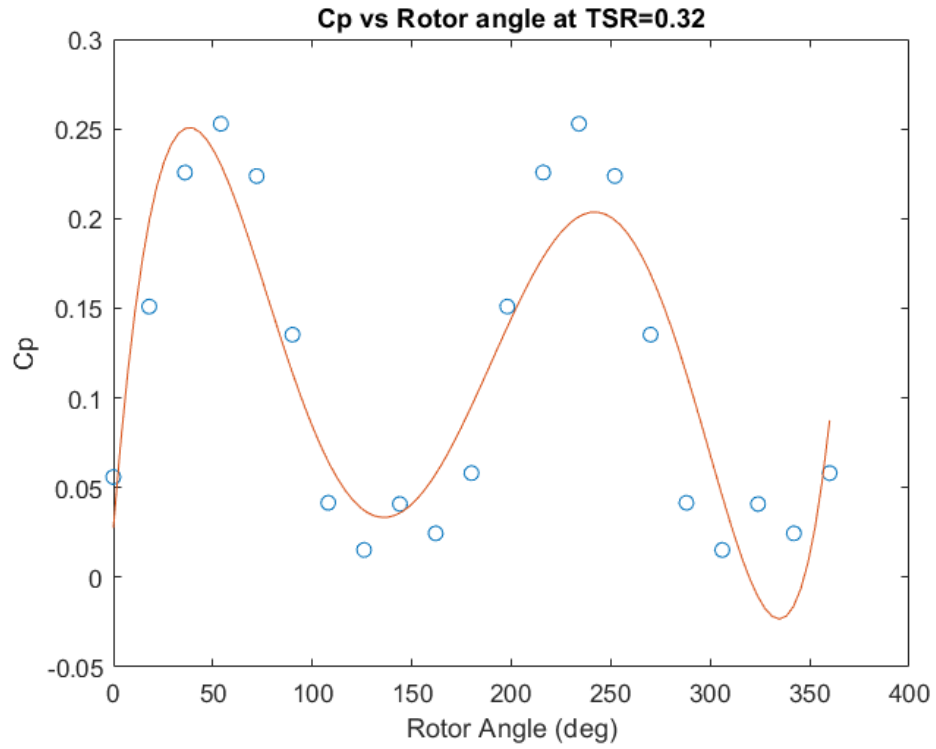

Figure 5.15: Variation of Power coefficient at different rotor angles at TSR=0.32

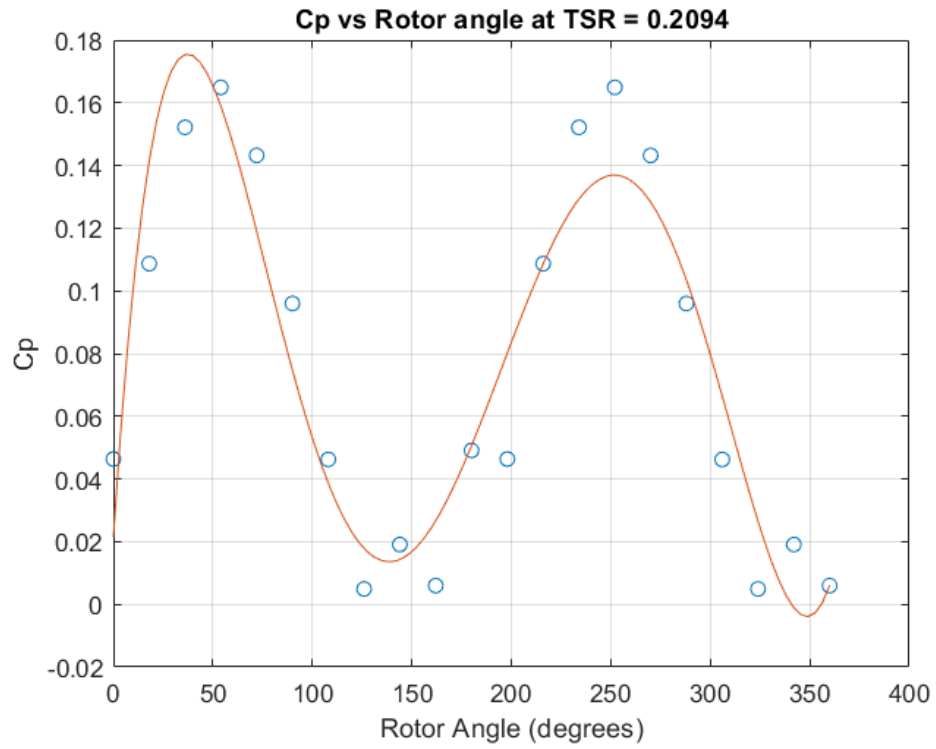

Figure 5.16: Variation of Power coefficient at different rotor angles at TSR=0.2094

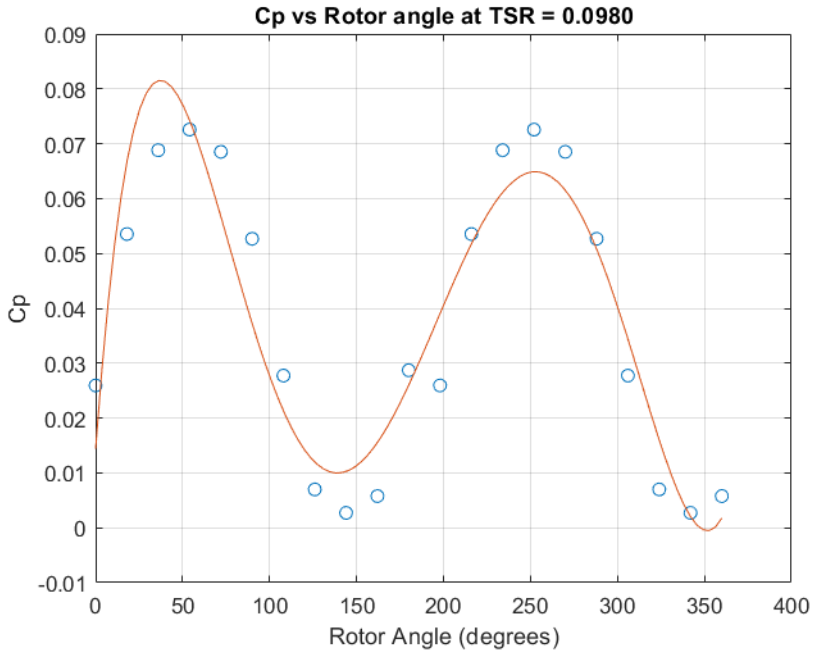

Figure 5.17: Variation of Power coefficient at different rotor angles at TSR=0.0988

Table 5.1: Test Data 1

Wind speed(m/s)	RPM	W1 (Spring)	W2	Difference
3.3	44.5	2.61	0.505	2.105
3.4	45.8	2.54	0.505	2.035
3.5	44.3	3.015	0.505	2.51
3.6	44.6	2.575	0.505	2.07
	44.7	2.54	0.505	2.035

Table 5.2: Test Data 2

Wind speed(m/s)	RPM	W1 (Spring)	W2	Difference
4.1	48	2.43	0.305	2.125
4.2	48.1	3.015	0.505	2.51
	48.7	2.86	0.505	2.355
	47.9			
	48.2			

Table 5.3: Test Data 3

Wind speed(m/s)	RPM	W1 (Spring)	W2	Difference
3.61	43	2.8	0.505	2.295
3.81	47.4	2.42	0.505	1.915
3.91	48.3	2.645	0.505	2.14
4.2	48.9	2.87	0.505	2.365

Table 5.4: Test Data 4

Wind speed(m/s)	RPM	W1 (Spring)	W2	Difference
2.9	39.3	2.765	0.705	2.06
3.0	40.02	2.095	0.505	1.59
2.7	40.02	2.185	0.505	1.68
3.4	39.2	2.43	0.505	1.925
3.1	39.3			
3.0	39.2			

Table 5.5: Test 5

Wind speed(m/s)	RPM	W1(Spring)	W2	Difference
2.5	32.5	1.65	0.505	1.145
2.7	32.9	2.125	0.505	1.62
2.2	31.6	2.62	0.705	1.915
2.4	31.1	2.635	0.705	1.93
	31.8	2.41	0.505	1.905
	31	2.305	0.505	1.8
	33.4	2.275	0.505	1.77
	32.1	2.01	0.505	1.505
	32.5	2.325	0.505	1.82

Table 5.6: Test Data 6

Wind speed(m/s)	RPM	W1(Spring)	W2	Difference
1.9	23.1	2.685	0.705	1.98
2.1	23.01	2.425	0.705	1.72
1.7	23.5	2.045	0.705	1.34
2	22.6	2.69	0.705	1.985
1.8		2.345	0.705	1.64
		0.93	0.505	0.425
		1.045	0.505	0.54
		1.01	0.505	0.505
		1.335	0.505	0.83
		2.14	0.505	1.635
		2.075	0.505	1.57
		2.175	0.505	1.67

Table 5.7: Test Data 7

Wind speed(m/s)	RPM	W1(Spring)	W2	Difference
1.4	20.3	1.215	0.505	0.71
1.5	19.6	1.2	0.505	0.695
1.6	19.8	1.62	0.505	1.115
1.41	20	1.55	0.505	1.045
1.7		1.085	0.505	0.58
1.5		1.065	0.505	0.56
1.5				
1.6				

Table 5.8: Test Data 8

Wind speed(m/s)	RPM	W1(Spring)	W2	Difference
1	15.593447	0.86	0.505	0.355
1.1	15.593447	0.93	0.505	0.425
1.2	15.593447	0.895	0.505	0.39

Wind Speed(m/s)	**RPM**	**W1(kg)(Spring)**	**W2(kg)(Dead Weight)**	**Difference(kg)**
4.0	48.87	3.51	0.705	2.80
4.0	24.96	1.71	0.205	1.505
4.0	16.24	2.37	0.305	2.07
4.0	7.667	2.933	0.405	2.528

Table 5.9: Test data at wind speed of 4 m/s at various rotational speed(TSRs)

Design and Fabrication of Savonius Wind Turbine and Experimental Study of its Use in a Water Pump

ORIGINALITY REPORT

8%
SIMILARITY INDEX

PRIMARY SOURCES

1	A. Damak, Z. Driss, M.S. Abid. "Optimization of the helical Savonius rotor through wind tunnel experiments", Journal of Wind Engineering and Industrial Aerodynamics, 2018 Crossref	86 words — 1%
2	Ahmad, Elsadic Salim. "A Study of the Influence of Guide Vane Design to Increase Savonius Wind Turbine Performance", Modern Applied Science, 2015. Crossref	82 words — 1%
3	dokumen.pub Internet	54 words — 1%
4	Craig MacEachern, İlhami Yıldız. "1.16 Wind Energy", Elsevier BV, 2018 Crossref	43 words — < 1%
5	mdpi-res.com Internet	43 words — < 1%
6	Ahmed Saad, Ali AbdelSalam, I. Sakr, W. El-Askary. "Performance Analysis of a Helical Savonius Wind Turbine with Modified Rotor", International Conference on Aerospace Sciences and Aviation Technology, 2017 Crossref	41 words — < 1%

7	M.A. Kamoji, S.B. Kedare, S.V. Prabhu. "Performance tests on helical Savonius rotors", Renewable Energy, 2009 Crossref	31 words — < 1%
8	www.tandfonline.com Internet	31 words — < 1%
9	Sohrabi, Azadeh. "A Computational Analysis to Investigate the Aerodynamic Performance of Horizontal Axis Wind Turbines", State University of New York at Buffalo, 2023 ProQuest	29 words — < 1%
10	Ahmad Zakaria, M S N Ibrahim. "Effect of twist angle on starting capability of a Savonius rotor – CFD analysis", IOP Conference Series: Materials Science and Engineering, 2020 Crossref	23 words — < 1%
11	Arteaga López Ernesto. "Metodología para la optimización del uso del recurso eólico aplicando análisis de dinámica de fluidos computacional para la instalación de aerogeneradores de baja potencia en zonas urbanas y rurales", TESIUNAM, 2020 Publications	22 words — < 1%
12	eprints.utem.edu.my Internet	21 words — < 1%
13	Jeon, Keum Soo, Jun Ik Jeong, Jae-Kyung Pan, and Ki-Wahn Ryu. "Effects of end plates with various shapes and sizes on helical Savonius wind turbines", Renewable Energy, 2015. Crossref	20 words — < 1%

14	Lakshmi Srinivasan, Nishanth Ram, Sudharshan Bharatwaj Rengarajan, Unnikrishnan Divakaran et al. "Effect of Macroscopic Turbulent Gust on the Aerodynamic Performance of Vertical Axis Wind Turbine", Energies, 2023 Crossref	19 words — < 1%
15	M. Elkhoury, T. Kiwata, K. Nagao, T. Kono, F. ElHajj. "Wind tunnel experiments and Delayed Detached Eddy Simulation of a three-bladed micro vertical axis wind turbine", Renewable Energy, 2018 Crossref	18 words — < 1%
16	www.iao.florence.it Internet	17 words — < 1%
17	eprints.hud.ac.uk Internet	16 words — < 1%
18	Y.B. Lukiyanto. "A Couple of Savonius Wind Mill and Centrifugal Reaction Pump as a Wind Energy Water Pump System", Applied Mechanics and Materials, 2016 Crossref	14 words — < 1%
19	research.aalto.fi Internet	13 words — < 1%
20	Alfred J. Cavallo. "Wind energy: Current status and future prospects", Science & Global Security, 1993 Crossref	12 words — < 1%
21	COMPEL: The International Journal for Computation and Mathematics in Electrical and Electronic Engineering, Volume 33, Issue 5 (2014-09-16) Publications	11 words — < 1%

22	Yuhang Guo. "Analysis of Aerodynamic Loads on Wind Turbine Blades Based on Blade Element Momentum Theory and Machine Learning", 2021 IEEE 4th International Conference on Automation, Electronics and Electrical Engineering (AUTEEE), 2021 Crossref	11 words —	< 1%
23	pulptastic.com Internet	11 words —	< 1%
24	"Fluid Mechanics and Fluid Power (Vol. 2)", Springer Science and Business Media LLC, 2023 Crossref	10 words —	< 1%
25	Kamal Abdel Radi Ismail, Thiago Canale, Fatima A. M. Lino. "Parametric analysis of Joukowski airfoil for 10-kW horizontal axis windmill", Journal of the Brazilian Society of Mechanical Sciences and Engineering, 2018 Crossref	10 words —	< 1%
26	Lee, Jae-Hoon, Young-Tae Lee, and Hee-Chang Lim. "Effect of twist angle on the performance of Savonius wind turbine", Renewable Energy, 2016. Crossref	10 words —	< 1%
27	academic.oup.com Internet	10 words —	< 1%
28	openaccess.iyte.edu.tr Internet	10 words —	< 1%
29	theses.gla.ac.uk Internet	10 words —	< 1%
30	www.jetir.org Internet	10 words —	< 1%

31	Cameron Gerrie, Sheikh Zahidul Islam, Sean Gerrie, Naomi Turner, Taimoor Asim. "3D CFD Modelling of Performance of a Vertical Axis Turbine", Energies, 2023 Crossref	9 words — < 1%
32	Khader, Mohamed Farmaan Abdul. "Computational Performance Assessment of Buoyant Shrouded Turbines in UAE", Rochester Institute of Technology, 2023 ProQuest	9 words — < 1%
33	M.A. Kamoji, S.B. Kedare, S.V. Prabhu. "Experimental Investigations on Two and Three Stage Modified Savonius Rotor", Wind Engineering, 2011 Crossref	9 words — < 1%
34	W.A. El-Askary, Ahmed S. Saad, Ali M. AbdelSalam, I.M. Sakr. "Investigating the performance of a twisted modified Savonius rotor", Journal of Wind Engineering and Industrial Aerodynamics, 2018 Crossref	9 words — < 1%
35	academic.hep.com.cn Internet	9 words — < 1%
36	ir.aiktclibrary.org:8080 Internet	9 words — < 1%
37	www.tutorialspoint.com Internet	9 words — < 1%

EXCLUDE QUOTES	ON	EXCLUDE SOURCES	< 6 WORDS
EXCLUDE BIBLIOGRAPHY	ON	EXCLUDE MATCHES	< 9 WORDS